# Title:

The magnitude of sex differences in host-microbe interactions are time-of-day dependent


## Authors:

Sarah K. Munyoki[1-3], Julie P. Goff[1-3], Steven J. Mullett[4-5], Jennifer K. Burns[7,8], Aaron K. Jenkins[7,8], Lauren DePoy[7,8], Stacy G. Wendell[4-6], Colleen A. McClung[7-9], Kathleen E. Morrison[10], Eldin Jašarević[1-3] *

## Affiliations:

1. Department of Obstetrics, Gynecology and Reproductive Sciences, University of Pittsburgh School of Medicine, Pittsburgh, PA
2. Department of Computational and Systems Biology, University of Pittsburgh School of Medicine, Pittsburgh, PA
3. Magee-Womens Research Institute, Pittsburgh, PA
4. Department of Pharmacology & Chemical Biology, University of Pittsburgh School of Medicine, Pittsburgh, PA
5. Health Sciences Mass Spectrometry Core, University of Pittsburgh School of Medicine, Pittsburgh, PA
6. Clinical Translational Science Institute, University of Pittsburgh School of Medicine, Pittsburgh, PA
7. Department of Psychiatry, University of Pittsburgh School of Medicine, Pittsburgh, PA
8. Center for Neuroscience, University of Pittsburgh School of Medicine, Pittsburgh, PA
9. Clinical and Translational Science Institute, University of Pittsburgh School of Medicine, Pittsburgh, PA
10. Department of Psychology, West Virginia University, Morgantown, WV



**KEYWORDS:**

Circadian rhythms, sex differences, host-microbe interactions, microbial metabolites, integrative multi-Omics



*** To whom correspondence should be addressed:**

Eldin Jašarević, PhD
Assistant Professor
Department of Obstetrics, Gynecology and Reproductive Sciences
Department of Computational and Systems Biology
Magee-Womens Research Institute
University of Pittsburgh School of Medicine
204 Craft Avenue, B303
Pittsburgh, PA 15213

## SUMMARY

Circadian rhythms in microbial communities regulate a variety of essential homeostatic functions in the intestinal tract and distal tissues. Circadian disruption is often associated with sex-specific disease risk, but studies on circadian rhythms, the microbiome, and health outcomes primarily use male mice or collapse both sexes into one experimental condition. Here, we identify sex differences in diurnal rhythms in the intestinal microbiota, the metabolites they produce, and the expression of host genes, with more pronounced effects in females. The magnitude of these sex differences also varies by time of day, suggesting that time of collection may influence the capacity to detect sex differences in mice. Further, transitioning female mice to high-fat and low-fiber diet abolished circadian rhythms in microbiota, metabolites, and host gene expression that is entrained by a chow diet. As a result, consumption of a high-fat and low-fiber diet generated new diurnal rhythms in the microbiota and host transcriptome in females. Together, we show that circadian rhythms in the crosstalk between microbiota and their hosts are sex-specific and that diet plays an essential role in maintaining these sex differences.

## INTRODUCTION

Differences between females and males in anatomical, physiological, and behavioral traits have been described in all vertebrate species, including humans (Becker et al., 2007; Geary, 2010, 2016; Korstanje et al., 2004; Mackay, 2004; Ober et al., 2008; Ueno et al., 2004). Maintenance of such sex differences requires a delicate orchestration between genes, the endocrine system, and environmental factors across the distinct life history stages of males and females (Becker et al., 2007; Geary, 2010). A direct consequence of these biological sex differences is that diseases show a sex-specific bias in prevalence, age of onset, severity, and treatment outcome (Ober et al., 2008). For instance, women have an increased prevalence of autoimmune diseases, while a higher prevalence of cardiovascular disease is observed among men (Choi and McLaughlin, 2007; Lockshin, 2006). Despite clear links between sex-specific processes and lifelong health trajectories, their underlying molecular mechanisms have not yet been explored.

Accumulating evidence suggests that microbial communities within the intestinal tract play a key role in supporting sex differences in metabolism, immunity, and brain function (Jaggar et al., 2020; Jašarević et al., 2016). The composition of microbial communities in females and males are similar in early life, diverging around puberty, and these sex differences are maintained across adulthood (Yatsunenko et al., 2012). Sex-specific response to diet has been proposed as one crucial factor in driving these differences in microbial communities, as highlighted by recent work showing that gut microbiota respond to the same dietary challenge in a host sex-specific manner (Bolnick et al., 2014). The relative importance of environmental and dietary effects on gut microbial structure and function in the context of sex-specific susceptibility to disease and health outcomes remains poorly understood.

While the adult intestinal microbiota is often characterized by its long-term stability, recent work suggests that the relative abundance of microbiota shows significant variation across the span of twenty-four hours (Faith et al., 2013; Segers and Depoortere, 2021; Thaiss et al., 2014, 2016; Zarrinpar et al., 2016). Diurnal variation in microbiota abundance is synchronized with feeding rhythms and, together, controls a variety of essential homeostatic functions in the intestinal tract (Alvarez et al., 2020; Heinemann et al., 2021). Presence of a gut microbiota is necessary for entrainment of intestinal circadian rhythms, as highlighted by recent work showing that the microbiome coordinates with the circadian clock and feeding patterns to generate diurnal rhythms in energy homeostasis, lipid metabolism, and innate immune function (Brooks et al., 2021; Kuang et al., 2019; Wang et al., 2017). For instance, loss of circadian rhythms in microbial attachment to the intestinal epithelium prevents a release of antimicrobial peptides into the intestinal lumen, and, as a result, influences susceptibility to infection (Brooks et al., 2021).

Peripheral circadian rhythms also influence the composition of microbial communities in a sex-specific manner. Total bacterial load and microbial composition significantly change across the day and these diurnal shifts are more pronounced in female mice than male mice (Liang et al., 2015). Deletion of *Bmal1*, the principal driver of the mammalian molecular clock, abolishes differences in the microbiota composition between males (Liang et al., 2015). Additionally, sex differences in hepatic gene expression, metabolism, and reproductive development are disrupted in germ-free mice, suggesting that microbial-derived signals are necessary for sex-specific development and phenotype (Weger et al., 2019). How circadian variations in an intact microbiome contribute to sex-specific physiological processes is less well known. Individual variability in environmental and lifestyle exposures, including jet lag, shift work, antibiotic exposure, and altered feeding times or consumption of highly processed diets, are associated with disruption to diurnal rhythms in gut microbiota (Altaha et al., 2022; Dantas Machado et al., 2022; Leone et al., 2015; Thaiss et al., 2014;

Zarrinpar et al., 2014, 2018). In turn, microbial circadian misalignment is reported to increase the risk for obesity, poor glycemic control, metabolic dysfunction, inflammation, and overall heightened susceptibility to disease (Brooks and Hooper, 2020; Choi et al., 2021; Frazier and Chang, 2020; Penny et al., 2022; Zheng et al., 2020). Although circadian disruption is often associated with sex-specific health outcomes, most studies on circadian rhythms, the microbiome, and health outcomes use only male mice or collapse both sexes into one experimental condition (Walton et al., 2022).

Here, we sought to determine whether the microbial, metabolic, and transcriptional capacity in the intestinal tract show sex-specific circadian rhythms under normal feeding conditions. We specifically examined the central hypothesis that sex differences in host-microbe interactions are time-of-day-dependent. In addition, we determined whether chronic circadian disruption to feeding patterns through consumption of a high-fat low-fiber diet influence sex-specific synchronization of the microbiome, microbial metabolites, and host transcriptome. To test these hypotheses, we applied an integrated multi-Omics approach to identify sex differences in diurnal dynamics of the intestinal microbiota, production of microbial-derived metabolites, systemic availability of microbial metabolites, and the host transcriptome.

## RESULTS

### Cecal microbiota composition varies by sex and time-of-day.

A recent report showed that circadian rhythms in fecal microbiota are more pronounced in female mice than male mice (Liang et al., 2015). Informed by this work, we determined whether similar sex differences exist in the luminal content microbiota in the cecum, the intestinal region where most of the bacterial fermentation occurs, and a significant pool of the microbial metabolites short-chain fatty acids (SCFAs) are produced (Donaldson et al., 2016; Rooks and Garrett, 2016). To determine whether luminal microbiota show sex-specific diurnal rhythms, whole ceca were collected every 4h during a

24-h period from mice consuming a chow diet (calories provided by 23.2% protein, 55.2% carbohydrate, 21.6% fat; three female and male mice per time point). The community structure, diversity, and composition of luminal cecal microbiota was determined by amplifying the hypervariable V3-V4 region using 16S rRNA marker gene sequencing. Consistent with previous observations, the relative abundance of *Bacteroidota*, *Firmicutes*, *Verrucomicrobiota*, and *Deferribacterota* showed significant variation at Zeitgeber time (ZT) 12 and Z16 (where ZT0 is lights on and ZT12 is lights off) in the cecum of female and male mice (**Fig. 1A**) (Liang et al., 2015). A survey of the most abundant genera showed sex-specific differences in relative abundance across the day (**Fig. 1B**). Community alpha diversity, as measured by Shannon Diversity Index, showed sex-specific variation across the day at both phylum and genus taxonomic levels (**Fig. 1C**). In both cases, females had lower diversity than males during early periods of the behaviorally inactive phase (ZT0 to ZT4; $p < 0.01$), followed by a disappearance of sex differences between ZT8 to ZT16 ($p > 0.05$) due to increased microbial diversity in females. A later reestablishment of sex differences occurred at ZT20 to ZT24, driven by a diversity decrease in females ($p < 0.001$) (**Fig. 1C**).

As these results suggested that the magnitude of sex differences in community diversity and composition may vary across the day, we applied cosinor analysis to identify which taxa account for sex-specific rhythms (Cornelissen, 2014). The relative abundance of 54 of 293 (~17%) taxa oscillated in the cecum of females, while 46 of 306 (~15%) taxa showed diurnal variation in the cecum of males ($p < 0.05$ by Cosinor test) (**Fig. 1D**). We next fitted the cosinor regressions for each taxon to derive estimated acrophases, defined as the time-of-day that reflects peak relative abundance (**Fig. 1E**). The distribution of acrophases was localized to two time periods in females (ZT12 to ZT18, and ZT0 to ZT4), while acrophase distribution in males was extended across multiple time points (**Fig. 1E).** Of the microbiota whose relative abundance oscillated across the day, 14 showed similar

patterns in males and females (**Fig. 1F**). This suggests that sex differences cecal microbiota involve both differences in oscillating microbiota and the phase distribution of these rhythms across the day.

Previous work has shown that food-related cues, such as cyclic availability of dietary-derived nutrients, exert strong effects on microbial composition and function (Brooks et al., 2021; Thaiss et al., 2014). Based on this work, several predictions can be generated for day-night variation in feed rhythms and nutrient availability in driving microbial rhythmicity: 1) microbiota that may show peak relative abundance during maximal nutrient availability, 2) microbiota that may show peak relative abundance during minimal nutrient availability, and 3) microbiota that may show no change in relative abundance due to diurnal nutrient availability. Consistently, we detected sex-specific patterns that fit the three criteria: 1) The SCFA butyrate producer *Butyricicoccus* showed similar rhythmicity in males and females with peak abundance around ZT16 (main effect of time, $F_{6, 23}$ = 3.098, $p$ = 0.0226) (**Fig. 1G**). Segmented Filamentous Bacteria showed sex-specific rhythmicity (time*sex, $F_{6, 27}$ = 2.850, $p$ = 0.0279), with peak abundance occurring in females prior to males (ZT12 vs. ZT16, respectively) (**Fig. 1H**). Relative abundance of cecal *Mucispirillum* shows sex-specific rhythmicity (time*sex, $F_{6, 27}$ = 4.850, $p$ = 0.0018), with peak abundance in males at ZT20 (**Fig. 1I**). 2) *Prevotellaceae UCG 001* showed sex-specific rhythmicity (time*sex, $F_{6, 27}$ = 6.414, $p$ = 0.0004), whereby relative abundance is in anti-phase in males and females (**Fig. 1J**). *Alistipes* showed a male-specific increase during the behavioral inactive phase but not females (time*sex, $F_{6, 27}$ = 3.190, $p$ = 0.0169) (**Fig. 1K**). *Lactobacillus* showed peak abundance during the light phase, with females showing a higher overall abundance of this taxon (main effect of sex, $F_{, 27}$ = 4.762, $p$ = 0.0380) (**Fig. 1L**)). 3) Relative abundance of *Muribaculaceae* (formerly S24-7) is stable across time of day in males and females (all *p's* > 0.05) (**Fig. 1M**). Taken together, our observations suggest that the composition and diversity of cecal luminal microbiota shows temporal sex-specific rhythms, and that the magnitude of these sex differences varies by time-of-day.

172

173 **Local and systemic availability of microbial-derived metabolites varies by time-of-day**

174 **and differs by sex**

175 Our analysis detected sex-specific diurnal variation in microbiota involved in fermentation and
176 production of the microbial metabolites SCFAs (Geirnaert et al., 2014; Segers et al., 2019). This class of
177 metabolites are potent regulators of physiological and molecular processes, including constraining
178 inflammation, controlling neural circuits involved in feeding and satiety, and regulating gene
179 expression via histone post-translational modifications and inhibition of histone deacetylase activity
180 (Chang et al., 2014; De Vadder et al., 2014; Smith et al., 2013). To determine whether availability of
181 SCFAs showed variation in the cecum of males and females across the day, luminal cecal contents
182 were collected every 4 h during a 24-h period (three female and male mice per time point). Cecal
183 weight showed significant variation across the day in males and females, whereby cecal weight
184 significantly decreased between ZT8 and ZT12 and then recovered in females compared with males
185 (**Supplementary Fig. 1**). Absolute quantification in the SCFAs formate, acetate, propionate,
186 butyrate, valerate, and hexanoate was measured using LC-MS/MS (Han et al., 2015). Valerate and
187 hexanoate fell below our level of detection in this assay. Cecal SCFA absolute quantities were
188 normalized per gram body weight to control for sex differences in cecal SCFA concentration that
189 may be attributed to baseline sexual dimorphism in mouse body weight. Plasma SCFA absolute
190 quantities were reported as a concentration ( µg/mL) based on volume and thus does not change
191 with body weight.

192 We next sought to detect sex differences in diurnal variation of SCFAs. Total luminal SCFA
193 availability in the cecum was similar in males and females across the day (**Fig. 2A**). Availability of
194 butyrate showed significant diurnal variation in the cecum of females (Cosinor $p < 0.0001$) and
195 males (Cosinor $p = 0.0016$) (**Fig. 2C**). Peak availability of cecal butyrate was also similar between

196 females and males (ZT21.2 and ZT21.5, respectively) (**Supplementary Fig. 2**). The magnitude of
197 sex differences in availability of cecal butyrate changed across the day, with a sex difference
198 detected at ZT8 that later disappeared. Formate, acetate, and propionate were available in equal
199 quantities across the day in the female cecum (all Cosinor *p*s > 0.05) (**Fig. 2B, D, E**). Formate and
200 acetate were available in equal quantities across the day in male cecum (all Cosinor *p*s > 0.05) (**Fig.**
201 **2B, E**).

202 To determine whether SCFA availability in the cecum was synchronized with diurnal rhythms
203 in circulating SCFA availability, plasma samples were collected every 4h during a 24-h period (three
204 female and male mice per time point). Propionate was the only SCFA to show rhythmic availability in
205 plasma of females (Cosinor $p = 0.007$) (**Fig. 2F-J**). In contrast, acetate and butyrate showed
206 rhythmic availability in the plasma of males (acetate Cosinor $p = 0.029$; butyrate Cosinor $p = 0.0032$)
207 (**Fig. 2F-J**). We then integrated acrophase values from the microbiome and metabolite datasets to
208 examine correlations between peak abundance of specific taxa and peak availability of specific
209 SCFA. This analysis revealed that *Butyricicoccus* blooms prior to the peak availability of cecal
210 butyrate, followed by peak availability of plasma butyrate (**Fig. 2K**). The exact timing of these events
211 differed between males and females, suggesting synchronized sex-specific diurnal rhythms in
212 feeding patterns, microbial dynamics, and the subsequent local production and systemic availability
213 microbially derived metabolites.

214 Host genetics and housing conditions exhibit strong effects on the magnitude of sex
215 differences in mice (Jonasson, 2005; Org et al., 2016; Võikar et al., 2001). To determine whether our
216 observed sex differences in diurnal rhythms in microbiota and metabolites reflect a generalizable
217 pattern in mice, we repeated these experiments with BALB/c mice reared in a different animal
218 housing facility. Cosinor analysis revealed similar sex differences in cecal weight and diurnal
219 rhythms in cecal availability of SCFAs in BALB/c males and females (**Supplementary Fig. 4**).

Similarities in sex-specific diurnal rhythm in SCFA availability across mouse strains may suggest that these rhythms are evolutionary conserved in mice and warrants further investigation.

**The transcriptional landscape of the small intestine exhibits circadian rhythmicity that differs by sex**

Variation in microbial community composition and microbial metabolite availability influence transcriptional patterns in host tissues (Grieneisen et al., 2020; Richards et al., 2016, 2019). To determine whether diurnal variation in microbiota and microbial metabolites associate with sex-specific rhythmic expression of host genes, small intestinal ileum segments were collected every 4h during a 24-h period (three female and male mice per time point). We used cosinor analysis to detect oscillations in the ileum transcriptome datasets. We detected sex differences in the number of rhythmic transcripts. Females showed diurnal rhythms in 3492 transcripts (~24%) compared with 278 rhythmic transcripts (2%) in males ($p < 0.05$ by Cosinor test) (**Fig. 3A**). Females and males showed similar diurnal rhythms in only 53 transcripts, confirming presence of robust sex differences in the diurnal gene expression within the small intestine (**Fig. 3B**). Consistently, analyses of acrophases revealed sex-specific distribution pattern of peak gene expression. Females exhibit a higher number of genes peaking between ZT8 to ZT12 and ZT16 to ZT20 and males showed a higher number of genes peaking between ZT2 to ZT6 and ZT13 to ZT18 (**Fig. 3C, D**). An earlier onset and acrophase of feeding have been observed in females (~4 hours earlier than males), suggesting that these phase shifts in intestinal gene expression patterns may reflect sex differences in feeding rhythms and microbial dynamics (Chen et al., 2015).

To determine whether sex differences in rhythmic expression of transcripts map onto transcriptional networks and functional pathways. Acrophase values for each cycling gene were collapsed into 4-hour bins and then analyzed for statistical overrepresentation using Gene Ontology:

Biological Process terms (e.g., ZT0 to ZT4, ZT4 to ZT8, ZT8 to ZT12, ZT12 to ZT16, ZT16 to ZT20, ZT20 to ZT24). Analysis of female-specific cycling genes revealed significant enrichment of functional pathways across the day (all pathways FDR < 0.05) (**Supplementary Fig. 5**). Pathways involved in the response to hyperoxia, wound healing, and cholesterol import are enriched in the early behaviorally inactive phase (ZT0 - 4) (**Supplementary Fig. 5A**). Immune-related pathways such as mucosal immune responses, antigen processing, and immunoglobulin production are enriched in the late behaviorally inactive phase (ZT4 - 12) (**Supplementary Fig. 5B, C**). Consistent with adaptations related to onset of feeding in the early behaviorally active phase, enrichment of pathways involved in the regulation microvillus length, brush border assembly, intestinal absorption, intestinal cholesterol absorption, and fatty acid oxidation (**Supplementary Fig. 5D**). Pathways involved in chromatin remodeling, histone acetylation, histone methylation, and post-translational modification of histone residues were specifically enriched during ZT16 to ZT20, suggesting the possibility that peak expression of genes involved in chromatin remodeling exhibit important diurnal rhythmic in the small intestine of females (**Supplementary Fig. 5E**). Lastly, the late phase of the behaviorally active phase showed enrichment of pathways involved in leptin and insulin signaling (**Supplementary Fig. 5F**). Surprisingly, analysis in male-specific cycling genes revealed no significant overrepresentation in specific biological processes across all time bins examined, likely due to the limited number of cycling genes detected by cosinor analysis. Together, our data support the hypothesis that diurnal variations in microbiota and their metabolites may be associated with sex differences in diurnal transcriptional patterns in the intestinal tract.

**Circadian rhythms in microbiota and metabolites are disrupted by consumption of a high-fat low-fiber diet in females**

Consumption of a high-fat low-fiber diet is associated with a shift in diurnal feeding patterns, resulting in mice consuming most calories during the behaviorally inactive phase (Kohsaka et al., 2007). These altered feeding patterns are associated with circadian disruption in hepatic homeostasis, increased body weight gain, poor glycemic control, and low-grade inflammation in male mice (Chaix et al., 2014; Gachon et al., 2018; Hatori et al., 2012). Consumption of a high-fat low-fiber diet also disrupts circadian rhythms of the gut microbiota and host genes in male mice (Dantas Machado et al., 2022; Leone et al., 2015; Zarrinpar et al., 2014). Building on our results showing more significant amplitudes in the oscillations of microbiota in females, we next determined the influence of diet-mediated circadian disruption on microbial composition and metabolite availability in female mice (**Fig. 4A**). Pubertal females were randomly assigned to either high-fat low-fiber diet (calories provided by 20% protein, 20% carbohydrate, 60% fat) or a chow diet (calories provided by 23.2% protein, 55.2% carbohydrate, 21.6% fat) (Gohir et al., 2019; Jašarević et al., 2021). An important note on treatment group notation: We explicitly highlight the absence of soluble fiber in commercially available refined high-fat diet formulations due to accumulating evidence that the lack of soluble fiber in these dietary formulations is an important contributor to excessive weight gain, obesity, and diabetes in mouse models of diet-induced metabolic syndrome and obesity (Chassaing et al., 2015; Dalby et al., 2017; Jašarević et al., 2021; Morrison et al., 2020; Pellizzon and Ricci, 2018, 2020). Females had *ad libitum* access to respective diets for the duration of the experiment. Weekly body weights were recorded, and glycemic control was evaluated in adulthood. This feeding paradigm produced a phenotype characterized by excessive body weight gain and delayed glucose clearance relative to females consuming a chow diet (Jašarević et al., 2021).

We next determined whether consumption of a high-fat low-fiber diet influenced diurnal rhythms in the intestinal microbiota, and SCFA availability. For microbiome and metabolite analyses, whole ceca were collected every 4 h during a 24-h period (three females per diet and time point).

Consumption of a high-fat low-fiber diet disrupted the diurnal rhythms in microbial community composition observed in the female mice consuming a chow diet (**Fig. 4B, C**). Analysis of cecal microbial diversity, as measured by the Shannon Diversity Index, showed that consumption of a high-fat low-fiber diet was associated with a bloom in phyla Defferribacterota, Desulfobacterota, and Verrucomicrobiota in the early phase of the behaviorally inactive period (ZT0 to ZT8), indicative of circadian misalignment in these females. Owing to a reduction in the relative abundance of Muribaculaceae, community diversity was increased, and diurnal rhythms were disrupted in females consuming a high-fat low-fiber diet compared with females consuming a chow diet (**Fig. 4C, D**).

We next sought to identify diet-specific effects on rhythmic microbiota. The number of rhythmic microbiota was reduced from 51 to 11 in females consuming a high-fat low-fiber diet, with only one taxon showing similar rhythmic patterns between chow and high-fat low-fiber fed females (**Fig. 4E, F)**. Analysis of acrophase distributions revealed a loss of the diurnal chow diet pattern and a gain of rhythm characterized by peak relative abundance at ZT6 to ZT12 (**Fig. 4G**). At the taxonomic level, females consuming the high-fat low-fiber diet lost rhythmicity in *Butyricicoccus,* Segmented Filamentous Bacteria, and *Prevotellaceae UCG 001* but gained rhythmicity in three genera that are commonly associated with obesity, namely *Acetatifactor, Blautia, and Bilophila* (**Fig. 4H-L**). Recent work has shown that dietary lipids are required for the expansion of *Bilophila,* indicating that the presence of excess dietary fat in the high-fat low-fiber diet may explain the acquisition of a diurnal rhythm in *Bilophila* (Natividad et al., 2018). Further, gain of rhythmicity in *Acetatifactor, Blautia,* and *Bilophila* was not detected in a recent study examining the impact of diet-induced obesity on microbial diurnal rhythms in male mice, pointing to sex-specific effects of a high-fat low-fiber diet (Dantas Machado et al., 2022).

The parallel diurnal rhythm loss of SCFA producer *Butyricicoccus* and rhythmicity gain in SCFA producers *Acetatifactor* and *Blautia* suggests an alternate pathway for SCFA production in

the context of high-fat low-fiber feeding. Cosinor analysis of formate, butyrate, acetate, and propionate showed significant reduction and loss of rhythmicity in the cecum of females consuming a high-fat low-fiber diet compared with females consuming a chow diet (**Supplementary Fig. 6**). A similar decrease in the availability and loss of rhythmicity of formate, acetate, and propionate was observed in the plasma of females consuming a high-fat low-fiber diet. Although cecal butyrate availability was significantly reduced in high-fat low-fiber females, plasma butyrate concentration was indistinguishable from chow diet females, suggesting other sources of peripheral butyrate in female mice. To further clarify whether presence of a microbiome is necessary for peripheral availability of SCFAs, whole ceca from germ-free female mice were collected at ZT6, ZT10, ZT14 and ZT18 (**Supplementary Fig. 7**). Acetate, butyrate, and propionate were undetectable in the ceca of germ-free female mice while all SCFAs were present at detectable levels in the plasma of germ-free females. This may imply that a fraction of the total SCFA pool in circulation is derived independent of the presence of a microbiome in female mice (**Supplementary Fig. 7**).

**Circadian rhythms in host gene expression are disrupted by consumption of a high-fat low-fiber diet in females**

As our results showed synchronization between diurnal rhythms in microbial composition, metabolite availability and host gene expression patterns, we next determined whether acquisition of new rhythms in gut microbiota is associated with alterations to host gene expression patterns. Consistent with this hypothesis, cosinor analysis of ileal transcriptome data revealed that consumption of a high-fat low-fiber diet resulted in a ~80% reduction in the number of rhythmic transcripts (3492 to 573 transcripts) (**Fig. 5A**). Of the rhythmic transcripts, only 94 transcripts were shared between high-fat low-fiber and chow diet females, suggesting that the remaining 479 transcripts gained circadian oscillations (**Fig. 5B**). Analysis of acrophase distribution shows that the primary loss of

rhythmic transcripts occurred during the ZT18 to ZT24 (**Fig. 5C**). Surprisingly, analysis of cycling genes detected females consuming a high-fat low-fiber diet revealed no significant overrepresentation in specific biological processes across all time bins examined (FDR > 0.05). Additional analysis of candidate genes involved in regulation of the mammalian molecular clock (*Arntl, Rora, Nr1d1*), innate immunity (Tlr4, *Defa3*), energy metabolism (*Cd36*, *Lep, Irs1,* Hsd17b2), SCFA sensing (*Ffar2),* and histone post-translational modifications (*Brd3, Hdac10*) indicated that the loss of transcriptional diurnal rhythms was primarily driven by flattened amplitudes of cycling genes in females consuming a high-fat low-fiber diet compared with females consuming a chow diet (**Figure 5**). Conversely, genes involved in autophagy (*Ctsd*), aerobic respiration (Dld), histone ubiquitination (Paf1, Rnf2), and inflammatory responses (Il17rc, Card9) gained oscillations in females consuming a high-fat low-fiber diet compared with females consuming a chow diet (**Supplementary Figure 8A-F**). These newly acquired cycling genes had small amplitudes, suggesting that changes in the amplitude of cycling genes may occur within specific nutritional contexts (Wang et al., 2015). To determine whether diet composition influences the amplitudes of cyclic genes in the ileum, we calculated an amplitude ratio for every cycling gene that was shared between females consuming a chow or high-fat low-fiber diet. Of the 94 shared cycling genes, 21 genes showed higher amplitude in high-fat low-fiber females while the remaining 73 genes showed higher amplitude in the chow females (**Supplementary Figure 8G**). Paradoxically, while consumption of high-fat low-fiber diets is often described as reflecting a state of overnutrition and excess energy, our results suggest that the specific nutrients necessary for maintenance of high amplitudes are either lacking or partitioned elsewhere for other physiological processes (Ainge et al., 2011; Alfaradhi and Ozanne, 2011; Larter and Yeh, 2008; Stare, 1963). Taken together, these results show that consumption of a high-fat low-fiber diet disrupts rhythms in microbiota, microbial metabolites,

and host gene expression that is associated with consumption of a chow diet, and, in turn, establishes new rhythms in microbiota and expression of host genes.

## DISCUSSION

Sex differences in homeostatic functions are essential for life-long health trajectories, whereby disruption is associated with sex-specific risk for metabolic, immune, and neural diseases (Ober et al., 2008). Emerging evidence suggests that the gut microbiome may play a key role in meeting the divergent metabolic and immunologic demands of males and females (Jaggar et al., 2020; Jašarević et al., 2016). These microbial communities show significant shifts across time-of-day, and disruption to these circadian rhythms is associated with increased risk for metabolic dysfunction and inflammation(Alvarez et al., 2020; Brooks and Hooper, 2020; Choi et al., 2021; Zarrinpar et al., 2016; Zheng et al., 2020). Although circadian disruption is often associated with sex-specific health outcomes, studies on circadian rhythms, the microbiome, and health outcomes commonly use only male mice or collapse both sexes into one experimental condition (Walton et al., 2022). To address this potential gap in our knowledge, we determined whether the microbial, metabolic, and transcriptional capacity in the intestinal tract show sex-specific circadian rhythms. Additionally, we examined the female-specific impact of diet on host-microbe interactions across time-of-day.

We first determined whether the relative abundance of microbiota fluctuates across time-of-day in a sex-specific manner. Our analyses focused on the cecal luminal microbiota given the essential role of this community in digesting and producing key microbial substrates important for metabolism (Donaldson et al., 2016). Consistent with earlier studies examining the fecal microbiota (Liang et al., 2015), we observed significant sex differences in the diurnal rhythms in the diversity and composition of microbial communities. These sex differences were not uniform across the day, rather, the magnitude of difference between females and males was dependent on time-of-day. For

instance, the relative abundance of Segmented Filamentous Bacteria (SFB) was higher in females at ZT12 (e.g., 1800 EST) and males catch up by ZT16. This rhythmic abundance in SFB drives diurnal rhythms in the expression of antimicrobial peptides as an anticipatory cue for food and exposure of exogenous microbiota during the behaviorally active phase (Brooks et al., 2021). Considering these observations, our results may suggest that sex differences in SFB abundance may reflect sex differences in feeding rhythms. Indeed, a recent report showed that females begin to eat about two hours prior to lights off, resulting in earlier onset and peak of the feeding rhythm and a phase advancement in overall host-microbe interactions (Chen et al., 2015).

Consistent with the notion that feeding rhythms influence sex differences in microbiota, we also observed sex-specific microbial dynamics during the fasting period that occurs during the behaviorally inactive phase. The relative abundance of *Alistipes* and *Prevotellaceae UCG 001* is increased during the early behaviorally inactive phase in males but not females, while both sexes showed increased abundance of Lactobacillus. The diurnal rhythm and acrophase in the relative abundance of microbiota also influenced oscillations of microbial metabolites in the cecum and circulation. For instance, a peak in the relative abundance of *Butyricicoccus* preceded peak availability of the SCFA butyrate in the cecum, followed by peak availability of plasma butyrate six hours later. Collectively, the results of these studies reconstruct some of the sex-specific temporal dynamics in host feeding rhythms, microbial dynamics, and availability of microbial metabolites in circulation. As microbial metabolites influence a variety of distal tissues, incorporating time-of-day effects on microbiome-metabolite interactions may reveal novel epigenetic, metabolic, and immune associations involved in health and disease.

Natural variations in microbial composition and microbial metabolite availability play a significant role in regulating expression of host genes (Richards et al., 2019). We found that diurnal rhythms in the microbiome and its metabolites were associated with similar patterns in gene

expression and transcriptional networks. Unlike males, females showed stepwise changes in the transcriptional networks across the day, showing time-of-day shifts from pathways involved in defense mechanisms to cholesterol and lipid absorption and epigenetic processes. These distinct shifts in transcriptional networks may reflect the ways in which physiological processes in the intestinal tract are partitioned over the course of the day.

Borne out of these studies is a central question regarding the evolutionary origins of sex differences in host-microbe interactions. Life history theory offers explanations for the evolutionary pressures that shape the timing of life events in males and females (Cole, 1954; Hill and Kaplan, 1999; Partridge and Harvey, 1988; Stearns, 1989). A specific focus of life history theory is on defining age-schedules of growth, fertility, senescence, and mortality (Cole, 1954; Hill and Kaplan, 1999; Partridge and Harvey, 1988; Stearns, 1989). As individuals grow and then reproduce, increasing quantities of energy are required to balance homeostatic processes and reproduction. Thus, the timing of life events, such as growth, maturation, and reproduction, depends on the ecology of energy substrate availability and production (Cole, 1954; Eric Charnov, 1993; Partridge and Harvey, 1988; Roff, 1993; Stearns, 1989; West-Eberhard, 1989). From the perspective of life history trade-offs, individuals cannot continuously support all biological functions as the energy costs are too high. Circadian rhythms enable individuals to partition and prioritize energy allocation towards life-history events relative to predictable fluctuations in environmental conditions, such as daily fluctuations in food availability (Martinez-Bakker and Helm, 2015). Given the essential role of the microbiome in harvesting energy, recent efforts to integrate the microbiome into life history evolution propose that the composition and activity of microbial communities set the pace and timing of life history transitions (Metcalf et al., 2019; Turnbaugh et al., 2006). This idea is supported by reports showing that abrupt changes to microbial composition and function coincide with the changes in energy allocations required to transition across development, reproduction, and senescence (Al Nabhani et al., 2019; Jašarević et al., 2017;

Yatsunenko et al., 2012). In this light, sex-specific circadian rhythms in host-microbe interactions may be one proximate mechanism that links environmental factors such as food availability to the unique energy demands of female and male life histories.

Another important question concerns the role of diet and the energetic costs needed for the sex-specific maintenance of oscillations in microbes, metabolites, and host genes. Earlier work highlighted that both the nutritional composition of diets and timing of specific nutrient intake organize and entrain peripheral circadian rhythms in rodents and humans (Potter et al., 2016). For instance, shifting animals from a low-protein, high-carbohydrate diet to a high-protein, low-carbohydrate diet resulted in changes to the rhythmic expression of genes involved in gluconeogenesis in the mouse kidney and liver (Oishi et al., 2012). Similarly, switching human participants from a high-carbohydrate and low-fat diet to an isoenergetic diet composed of low-carbohydrate and high-fat increased the amplitude of rhythmic expression of genes involved in inflammation and metabolism (Pivovarova et al., 2015). One extrapolation of this work is that timing of feeding patterns and the nutritional composition of diets function as entrainment signals for host-microbe interactions. Microbial communities show preferences towards distinct dietary components, including protein, fiber, lactate, and urea (Zeng et al., 2022). Proportional changes to the availability of these nutrients results in an ecological advantage for bacteria that are supplied with their preferred substrate (Zeng et al., 2022). From this perspective, it is not surprising that transitioning females from a chow to a high-fat low-fiber diet eliminated circadian rhythms that are entrained by the consumption of a chow diet. Loss of rhythmicity occurred in microbiota and microbial metabolites that utilize soluble fiber, which may suggest that the parallel loss of rhythmicity in host genes is related to decreased availability of soluble fiber and warrants further study (Geirnaert et al., 2014)

Conversely, the modulation of dietary fat and soluble fiber initiated rhythmic oscillations of *Blautia* and *Bilophila*, a genus that favors dietary lipids for growth and expansion (Natividad et al.,

2018). We observed a similar gain-of-rhythmicity pattern in the ileal transcriptome of females consuming the high-fat low-fiber diet. Interestingly, the amplitudes of these newly cycling genes remained small. Amplitudes of cycling genes are influenced by host metabolic conditions, such that high nutrient flux results in large amplitudes while low nutrient flux results in small amplitudes (Wang et al., 2015). While animals consuming a high-fat low-fiber diet are commonly described as being in a state of excess energy and overnutrition, our results may suggest that such diets lack the nutrients or energy substrates for supporting oscillating genes with large amplitudes (Alfaradhi and Ozanne, 2011; Fleming et al., 2018; Stare, 1963). Thus, identification of specific nutrients necessary for supporting large amplitudes in cycling genes involved in homeostatic processes may provide key insight into novel approaches for the restoration of circadian rhythms and warrants further study.

Lastly, our studies may provide some practical considerations for the study of sex differences in preclinical and clinical settings. Homeostatic and biological functions vary across time of day, and our results show that when these processes are assessed may affect whether sex differences are detected (Nelson et al., 2021, 2022). Our reconstruction of some, but certainly not all, sex differences in the onset, acrophase, and amplitude of circadian rhythms in host-microbe interactions may provide guidance in selecting the right time of day to collect data. Moreover, crosstalk between microbiota and their hosts has far-reaching effects on health and disease trajectories (Belkaid and Hand, 2014; Collins and Belkaid, 2022; Helmink et al., 2019; Kostic et al., 2014; McDonald and McCoy, 2019; Round and Mazmanian, 2009). Additional experiments are now needed to consider sex differences in circadian rhythms of host-microbe interactions, and the ways in which disruption to these processes influence sex-specific disease risk. In all, our data highlights the importance of investigating sex differences in circadian rhythms across the microbiome, metabolites, and expression of host genes and how a better understanding of these fundamental processes may provide novel insight into diseases process that show a significant sex-bias in onset, severity, and treatment outcomes.

## Acknowledgments

This work is supported by funding from the Eunice Kennedy Shriver National Institute of Child Health and Human Development grants T32HD087194 (PI: SKM) Pilot Project from P50HD096723 (PI: EJ), the National Institute of Diabetes and Digestive and Kidney Diseases grant K0DK1121734 (PI: EJ), a Magee Auxiliary Research Scholars Award (PI: EJ) and Start Up funds from Magee-Womens Research Institute. The Health Sciences Metabolomics and Lipidomics Core is supported by grant S10OD023402 (PI: SGW). We acknowledge Timothy Hand, Jacob DeSchepper, Javonn Musgrove in the University of Pittsburgh Gnotobiotic Animal Studies Facility for technical assistance with circadian collections of germ-free mouse tissues. We acknowledge Will MacDonald in the Children's Hospital of Pittsburgh Health Sciences Sequencing Core for technical assistance with bulk RNA sequencing on the NextSeq 2000. We acknowledge Heather Evers, Cheyenne Miller, Heather Seiple, Aaron Siegel in the Magee-Womens Research Institute animal facility for technical assistance in care of mice. We acknowledge the University of Pittsburgh Center for Research Computing through the resources provided. Specifically, this work used the HTC cluster, which is supported by NIH award number S10OD028483.

## Author Contributions

Conceptualization, S.K.M., J.P.G., K.E.M., and E.J.; methodology, investigation, and validation, S.K.M., S.J.M., J.P.G., J.K.B., and A.J.K; formal analysis, S.K.M. and E.J.; resources, T.W.H., C.A.M., S.G.W., and E.J.; data curation, S.K.M., J.P.G., and E.J.; writing – original draft, S.K.M., J.P.G., and E.J., writing – reviewing and editing, S.K.M., S.J.M., C.A.M., T.W.H., S.G.W., K.E.M., J.P.G., and E.J.; S.K.M. and E.J.; supervision, E.J.; project administration, J.P.G and E.J.; funding acquisition, E.J.

## Declaration of Interests

The authors have no competing interests.

## Inclusion and Diversity

One or more of the authors of this paper self-identifies as an underrepresented ethnic minority in their field of research or within their geographical location. One or more of the authors of this paper self-identifies as a member of the LGBTQIA+ community. One or more of the authors of this paper received support from a program designed to increase minority representation in their field of research. While citing references scientifically relevant for this work, we also actively worked to promote gender and racial balance in our reference list.

## References

Ainge, H., Thompson, C., Ozanne, S.E., and Rooney, K.B. (2011). A systematic review on animal models of maternal high fat feeding and offspring glycaemic control. Int J Obes *35*, 325-335. https://doi.org/10.1038/ijo.2010.149.

Al Nabhani, Z., Dulauroy, S., Marques, R., Cousu, C., Al Bounny, S., Déjardin, F., Sparwasser, T., Bérard, M., Cerf-Bensussan, N., and Eberl, G. (2019). A Weaning Reaction to Microbiota Is Required for Resistance to Immunopathologies in the Adult. Immunity *50*, 1276-1288.e5. https://doi.org/10.1016/j.immuni.2019.02.014.

Alfaradhi, M., and Ozanne, S. (2011). Developmental Programming in Response to Maternal Overnutrition. Frontiers in Genetics *2*. .

Altaha, B., Heddes, M., Pilorz, V., Niu, Y., Gorbunova, E., Gigl, M., Kleigrewe, K., Oster, H., Haller, D., and Kiessling, S. (2022). Genetic and environmental circadian disruption induce metabolic impairment through changes in the gut microbiome. 2022.07.27.501612. https://doi.org/10.1101/2022.07.27.501612.

Alvarez, Y., Glotfelty, L.G., Blank, N., Dohnalová, L., and Thaiss, C.A. (2020). The Microbiome as a Circadian Coordinator of Metabolism. Endocrinology *161*, bqaa059. https://doi.org/10.1210/endocr/bqaa059.

Becker, J.B., Berkley, K.J., Geary, N., Hampson, E., Herman, J.P., and Young, E. (2007). Sex Differences in the Brain: From Genes to Behavior (Oxford University Press).

Belkaid, Y., and Hand, T.W. (2014). Role of the Microbiota in Immunity and Inflammation. Cell *157*, 121-141. https://doi.org/10.1016/j.cell.2014.03.011.

Bolnick, D.I., Snowberg, L.K., Hirsch, P.E., Lauber, C.L., Org, E., Parks, B., Lusis, A.J., Knight, R., Caporaso, J.G., and Svanbäck, R. (2014). Individual diet has sex-dependent effects on vertebrate gut microbiota. Nat Commun *5*, 4500. https://doi.org/10.1038/ncomms5500.

Brooks, J.F., and Hooper, L.V. (2020). Interactions among microbes, the immune system, and the circadian clock. Semin Immunopathol *42*, 697-708. https://doi.org/10.1007/s00281-020-00820-1.

Brooks, J.F., Behrendt, C.L., Ruhn, K.A., Lee, S., Raj, P., Takahashi, J.S., and Hooper, L.V. (2021). The microbiota coordinates diurnal rhythms in innate immunity with the circadian clock. Cell *184*, 4154-4167.e12. https://doi.org/10.1016/j.cell.2021.07.001.

Chaix, A., Zarrinpar, A., Miu, P., and Panda, S. (2014). Time-restricted feeding is a preventative and therapeutic intervention against diverse nutritional challenges. Cell Metab *20*, 991-1005. https://doi.org/10.1016/j.cmet.2014.11.001.

Chang, P.V., Hao, L., Offermanns, S., and Medzhitov, R. (2014). The microbial metabolite butyrate regulates intestinal macrophage function via histone deacetylase inhibition. Proceedings of the National Academy of Sciences *111*, 2247-2252. https://doi.org/10.1073/pnas.1322269111.

Chassaing, B., Miles-Brown, J., Pellizzon, M., Ulman, E., Ricci, M., Zhang, L., Patterson, A.D., Vijay-Kumar, M., and Gewirtz, A.T. (2015). Lack of soluble fiber drives diet-induced adiposity in mice. APSselect *2*, G528-G541. https://doi.org/10.1152/ajpgi.00172.2015@apsselect.2015.2.issue-11.

Chen, X., Wang, L., Loh, D.H., Colwell, C.S., Taché, Y., Reue, K., and Arnold, A.P. (2015). Sex differences in diurnal rhythms of food intake in mice caused by gonadal hormones and complement of sex chromosomes. Hormones and Behavior *75*, 55-63. https://doi.org/10.1016/j.yhbeh.2015.07.020.

Choi, B.G., and McLaughlin, M.A. (2007). Why men's hearts break: cardiovascular effects of sex steroids. Endocrinol Metab Clin North Am *36*, 365-377. https://doi.org/10.1016/j.ecl.2007.03.011.

Choi, H., Rao, M.C., and Chang, E.B. (2021). Gut microbiota as a transducer of dietary cues to regulate host circadian rhythms and metabolism. Nat Rev Gastroenterol Hepatol *18*, 679-689. https://doi.org/10.1038/s41575-021-00452-2.

Cole, L.C. (1954). The Population Consequences of Life History Phenomena. The Quarterly Review of Biology *29*, 103-137. https://doi.org/10.1086/400074.

Collins, N., and Belkaid, Y. (2022). Control of immunity via nutritional interventions. Immunity *55*, 210-223. https://doi.org/10.1016/j.immuni.2022.01.004.

Cornelissen, G. (2014). Cosinor-based rhythmometry. Theoretical Biology and Medical Modelling *11*, 16. https://doi.org/10.1186/1742-4682-11-16.

Dalby, M.J., Ross, A.W., Walker, A.W., and Morgan, P.J. (2017). Dietary Uncoupling of Gut Microbiota and Energy Harvesting from Obesity and Glucose Tolerance in Mice. Cell Rep *21*, 1521-1533. https://doi.org/10.1016/j.celrep.2017.10.056.

Dantas Machado, A.C., Brown, S.D., Lingaraju, A., Sivaganesh, V., Martino, C., Chaix, A., Zhao, P., Pinto, A.F.M., Chang, M.W., Richter, R.A., et al. (2022). Diet and feeding pattern modulate diurnal dynamics of the ileal microbiome and transcriptome. Cell Reports *40*, 111008. https://doi.org/10.1016/j.celrep.2022.111008.

De Vadder, F., Kovatcheva-Datchary, P., Goncalves, D., Vinera, J., Zitoun, C., Duchampt, A., Bäckhed, F., and Mithieux, G. (2014). Microbiota-Generated Metabolites Promote Metabolic Benefits via Gut-Brain Neural Circuits. Cell *156*, 84-96. https://doi.org/10.1016/j.cell.2013.12.016.

Donaldson, G.P., Lee, S.M., and Mazmanian, S.K. (2016). Gut biogeography of the bacterial microbiota. Nat Rev Microbiol *14*, 20-32. https://doi.org/10.1038/nrmicro3552.

Eric Charnov (1993). Life History Invariants: Some Explorations of Symmetry in Evolutionary Ecology (Oxford, New York: Oxford University Press).

Faith, J.J., Guruge, J.L., Charbonneau, M., Subramanian, S., Seedorf, H., Goodman, A.L., Clemente, J.C., Knight, R., Heath, A.C., Leibel, R.L., et al. (2013). The Long-Term Stability of the Human Gut Microbiota. Science *341*, 1237439. https://doi.org/10.1126/science.1237439.

Fleming, T.P., Watkins, A.J., Velazquez, M.A., Mathers, J.C., Prentice, A.M., Stephenson, J., Barker, M., Saffery, R., Yajnik, C.S., Eckert, J.J., et al. (2018). Origins of lifetime health around the time of conception: causes and consequences. The Lancet *391*, 1842-1852. https://doi.org/10.1016/S0140-6736(18)30312-X.

Frazier, K., and Chang, E.B. (2020). Intersection of the Gut Microbiome and Circadian Rhythms in Metabolism. Trends Endocrinol Metab *31*, 25-36. https://doi.org/10.1016/j.tem.2019.08.013.

Gachon, F., Yeung, J., and Naef, F. (2018). Cross-regulatory circuits linking inflammation, high-fat diet, and the circadian clock. Genes Dev. *32*, 1359-1360. https://doi.org/10.1101/gad.320911.118.

Geary, D.C. (2010). Male, female: The evolution of human sex differences, 2nd ed (Washington, DC, US: American Psychological Association).

Geary, D.C. (2016). Evolution of Sex Differences in Trait- and Age-Specific Vulnerabilities. Perspect Psychol Sci *11*, 855-876. https://doi.org/10.1177/1745691616650677.

Geirnaert, A., Steyaert, A., Eeckhaut, V., Debruyne, B., Arends, J.B.A., Van Immerseel, F., Boon, N., and Van de Wiele, T. (2014). Butyricicoccus pullicaecorum, a butyrate producer with probiotic potential, is intrinsically tolerant to stomach and small intestine conditions. Anaerobe *30*, 70-74. https://doi.org/10.1016/j.anaerobe.2014.08.010.

Gohir, W., Kennedy, K.M., Wallace, J.G., Saoi, M., Bellissimo, C.J., Britz-McKibbin, P., Petrik, J.J., Surette, M.G., and Sloboda, D.M. (2019). High-fat diet intake modulates maternal intestinal adaptations to pregnancy and results in placental hypoxia, as well as altered fetal gut barrier proteins and immune markers. J Physiol *597*, 3029-3051. https://doi.org/10.1113/JP277353.

Grieneisen, L., Muehlbauer, A.L., and Blekhman, R. (2020). Microbial control of host gene regulation and the evolution of host-microbiome interactions in primates. Philosophical Transactions of the Royal Society B: Biological Sciences *375*, 20190598. https://doi.org/10.1098/rstb.2019.0598.

Han, J., Lin, K., Sequeira, C., and Borchers, C.H. (2015). An isotope-labeled chemical derivatization method for the quantitation of short-chain fatty acids in human feces by liquid chromatography-tandem mass spectrometry. Analytica Chimica Acta *854*, 86-94. https://doi.org/10.1016/j.aca.2014.11.015.

Hatori, M., Vollmers, C., Zarrinpar, A., DiTacchio, L., Bushong, E.A., Gill, S., Leblanc, M., Chaix, A., Joens, M., Fitzpatrick, J.A.J., et al. (2012). Time-restricted feeding without reducing caloric intake prevents metabolic diseases in mice fed a high-fat diet. Cell Metab *15*, 848-860. https://doi.org/10.1016/j.cmet.2012.04.019.

Heinemann, M., Ratiner, K., and Elinav, E. (2021). Basic Biology of Rhythms and the Microbiome. In Circadian Rhythms in Bacteria and Microbiomes, C.H. Johnson, and M.J. Rust, eds. (Cham: Springer International Publishing), pp. 317-328.

Helmink, B.A., Khan, M.A.W., Hermann, A., Gopalakrishnan, V., and Wargo, J.A. (2019). The microbiome, cancer, and cancer therapy. Nat Med *25*, 377-388. https://doi.org/10.1038/s41591-019-0377-7.

Hill, K., and Kaplan, H. (1999). Life History Traits in Humans: Theory and Empirical Studies. Annual Review of Anthropology *28*, 397-430. .

Jaggar, M., Rea, K., Spichak, S., Dinan, T.G., and Cryan, J.F. (2020). You've got male: Sex and the microbiota-gut-brain axis across the lifespan. Frontiers in Neuroendocrinology *56*, 100815. https://doi.org/10.1016/j.yfrne.2019.100815.

Jašarević, E., Morrison, K.E., and Bale, T.L. (2016). Sex differences in the gut microbiome-brain axis across the lifespan. Philos Trans R Soc Lond B Biol Sci *371*, 20150122. https://doi.org/10.1098/rstb.2015.0122.

Jašarević, E., Howard, C.D., Misic, A.M., Beiting, D.P., and Bale, T.L. (2017). Stress during pregnancy alters temporal and spatial dynamics of the maternal and offspring microbiome in a sex-specific manner. Sci Rep *7*, 44182. https://doi.org/10.1038/srep44182.

Jašarević, E., Hill, E.M., Kane, P.J., Rutt, L., Gyles, T., Folts, L., Rock, K.D., Howard, C.D., Morrison, K.E., Ravel, J., et al. (2021). The composition of human vaginal microbiota transferred at birth affects offspring health in a mouse model. Nat Commun *12*, 6289. https://doi.org/10.1038/s41467-021-26634-9.

Jonasson, Z. (2005). Meta-analysis of sex differences in rodent models of learning and memory: a review of behavioral and biological data. Neuroscience & Biobehavioral Reviews *28*, 811-825. https://doi.org/10.1016/j.neubiorev.2004.10.006.

Kohsaka, A., Laposky, A.D., Ramsey, K.M., Estrada, C., Joshu, C., Kobayashi, Y., Turek, F.W., and Bass, J. (2007). High-fat diet disrupts behavioral and molecular circadian rhythms in mice. Cell Metab *6*, 414-421. https://doi.org/10.1016/j.cmet.2007.09.006.

Korstanje, R., Li, R., Howard, T., Kelmenson, P., Marshall, J., Paigen, B., and Churchill, G. (2004). Influence of sex and diet on quantitative trait loci for HDL cholesterol levels in an SM/J by NZB/BlNJ intercross population. J Lipid Res *45*, 881-888. https://doi.org/10.1194/jlr.M300460-JLR200.

Kostic, A.D., Xavier, R.J., and Gevers, D. (2014). The Microbiome in Inflammatory Bowel Disease: Current Status and the Future Ahead. Gastroenterology *146*, 1489-1499. https://doi.org/10.1053/j.gastro.2014.02.009.

Kuang, Z., Wang, Y., Li, Y., Ye, C., Ruhn, K.A., Behrendt, C.L., Olson, E.N., and Hooper, L.V. (2019). The intestinal microbiota programs diurnal rhythms in host metabolism through histone deacetylase 3. Science *365*, 1428-1434. https://doi.org/10.1126/science.aaw3134.

Larter, C.Z., and Yeh, M.M. (2008). Animal models of NASH: Getting both pathology and metabolic context right. Journal of Gastroenterology and Hepatology *23*, 1635-1648. https://doi.org/10.1111/j.1440-1746.2008.05543.x.

Leone, V., Gibbons, S.M., Martinez, K., Hutchison, A.L., Huang, E.Y., Cham, C.M., Pierre, J.F., Heneghan, A.F., Nadimpalli, A., Hubert, N., et al. (2015). Effects of Diurnal Variation of Gut Microbes and High-Fat Feeding on Host Circadian Clock Function and Metabolism. Cell Host & Microbe *17*, 681-689. https://doi.org/10.1016/j.chom.2015.03.006.

Liang, X., Bushman, F.D., and FitzGerald, G.A. (2015). Rhythmicity of the intestinal microbiota is regulated by gender and the host circadian clock. Proc Natl Acad Sci U S A *112*, 10479-10484. https://doi.org/10.1073/pnas.1501305112.

Lockshin, M.D. (2006). Sex differences in autoimmune disease. Lupus *15*, 753-756. https://doi.org/10.1177/0961203306069353.

Mackay, T.F.C. (2004). The genetic architecture of quantitative traits: lessons from Drosophila. Curr Opin Genet Dev *14*, 253-257. https://doi.org/10.1016/j.gde.2004.04.003.

Martinez-Bakker, M., and Helm, B. (2015). The influence of biological rhythms on host-parasite interactions. Trends in Ecology & Evolution *30*, 314-326. https://doi.org/10.1016/j.tree.2015.03.012.

McDonald, B., and McCoy, K.D. (2019). Maternal microbiota in pregnancy and early life. Science *365*, 984-985. https://doi.org/10.1126/science.aay0618.

Metcalf, C.J.E., Henry, L.P., Rebolleda-Gómez, M., and Koskella, B. (2019). Why Evolve Reliance on the Microbiome for Timing of Ontogeny? MBio *10*, e01496-19. https://doi.org/10.1128/mBio.01496-19.

Morrison, K.E., Jašarević, E., Howard, C.D., and Bale, T.L. (2020). It's the fiber, not the fat: significant effects of dietary challenge on the gut microbiome. Microbiome *8*, 15. https://doi.org/10.1186/s40168-020-0791-6.

Natividad, J.M., Lamas, B., Pham, H.P., Michel, M.-L., Rainteau, D., Bridonneau, C., da Costa, G., van Hylckama Vlieg, J., Sovran, B., Chamignon, C., et al. (2018). Bilophila wadsworthia aggravates high fat diet induced metabolic dysfunctions in mice. Nat Commun *9*, 2802. https://doi.org/10.1038/s41467-018-05249-7.

Nelson, R.J., Bumgarner, J.R., Walker, W.H., and DeVries, A.C. (2021). Time-of-day as a critical biological variable. Neuroscience & Biobehavioral Reviews *127*, 740-746. https://doi.org/10.1016/j.neubiorev.2021.05.017.

Nelson, R.J., Bumgarner, J.R., Liu, J.A., Love, J.A., Meléndez-Fernández, O.H., Becker-Krail, D.D., Walker, W.H., Walton, J.C., DeVries, A.C., and Prendergast, B.J. (2022). Time of day as a critical variable in biology. BMC Biology *20*, 142. https://doi.org/10.1186/s12915-022-01333-z.

Ober, C., Loisel, D.A., and Gilad, Y. (2008). Sex-Specific Genetic Architecture of Human Disease. Nat Rev Genet *9*, 911-922. https://doi.org/10.1038/nrg2415.

Oishi, K., Uchida, D., and Itoh, N. (2012). Low-Carbohydrate, High-Protein Diet Affects Rhythmic Expression of Gluconeogenic Regulatory and Circadian Clock Genes in Mouse Peripheral Tissues. Chronobiology International *29*, 799-809. https://doi.org/10.3109/07420528.2012.699127.

Org, E., Mehrabian, M., Parks, B.W., Shipkova, P., Liu, X., Drake, T.A., and Lusis, A.J. (2016). Sex differences and hormonal effects on gut microbiota composition in mice. Gut Microbes *7*, 313-322. https://doi.org/10.1080/19490976.2016.1203502.

Partridge, L., and Harvey, P.H. (1988). The Ecological Context of Life History Evolution. Science *241*, 1449-1455. https://doi.org/10.1126/science.241.4872.1449.

Pellizzon, M.A., and Ricci, M.R. (2018). The common use of improper control diets in diet-induced metabolic disease research confounds data interpretation: the fiber factor. Nutr Metab (Lond) *15*, 3. https://doi.org/10.1186/s12986-018-0243-5.

Pellizzon, M.A., and Ricci, M.R. (2020). Choice of Laboratory Rodent Diet May Confound Data Interpretation and Reproducibility. Current Developments in Nutrition *4*, nzaa031. https://doi.org/10.1093/cdn/nzaa031.

Penny, H.A., Domingues, R.G., Krauss, M.Z., Melo-Gonzalez, F., Dickson, S., Parkinson, J., Hurry, M., Purse, C., Jegham, E., Godinho-Silva, C., et al. (2022). Rhythmicity of intestinal IgA responses confers oscillatory commensal microbiota mutualism. Science Immunology *7*. https://doi.org/10.1126/sciimmunol.abk2541.

Pivovarova, O., Jürchott, K., Rudovich, N., Hornemann, S., Ye, L., Möckel, S., Murahovschi, V., Kessler, K., Seltmann, A.-C., Maser-Gluth, C., et al. (2015). Changes of Dietary Fat and Carbohydrate Content Alter Central and Peripheral Clock in Humans. The Journal of Clinical Endocrinology & Metabolism *100*, 2291-2302. https://doi.org/10.1210/jc.2014-3868.

Potter, G.D.M., Cade, J.E., Grant, P.J., and Hardie, L.J. (2016). Nutrition and the Circadian System. Br J Nutr *116*, 434-442. https://doi.org/10.1017/S0007114516002117.

Richards, A.L., Burns, M.B., Alazizi, A., Barreiro, L.B., Pique-Regi, R., Blekhman, R., and Luca, F. (2016). Genetic and Transcriptional Analysis of Human Host Response to Healthy Gut Microbiota. MSystems *1*, e00067-16. https://doi.org/10.1128/mSystems.00067-16.

Richards, A.L., Muehlbauer, A.L., Alazizi, A., Burns, M.B., Findley, A., Messina, F., Gould, T.J., Cascardo, C., Pique-Regi, R., Blekhman, R., et al. (2019). Gut Microbiota Has a Widespread and Modifiable Effect on Host Gene Regulation. MSystems *4*, e00323-18. https://doi.org/10.1128/mSystems.00323-18.

Roff, D. (1993). Evolution Of Life Histories (Springer New York, NY).

Rooks, M.G., and Garrett, W.S. (2016). Gut microbiota, metabolites and host immunity. Nat Rev Immunol *16*, 341-352. https://doi.org/10.1038/nri.2016.42.

Round, J.L., and Mazmanian, S.K. (2009). The gut microbiota shapes intestinal immune responses during health and disease. Nat Rev Immunol *9*, 313-323. https://doi.org/10.1038/nri2515.

Segers, A., and Depoortere, I. (2021). Circadian clocks in the digestive system. Nat Rev Gastroenterol Hepatol *18*, 239-251. https://doi.org/10.1038/s41575-020-00401-5.

Segers, A., Desmet, L., Thijs, T., Verbeke, K., Tack, J., and Depoortere, I. (2019). The circadian clock regulates the diurnal levels of microbial short-chain fatty acids and their rhythmic effects on colon contractility in mice. Acta Physiol (Oxf) *225*, e13193. https://doi.org/10.1111/apha.13193.

Smith, P.M., Howitt, M.R., Panikov, N., Michaud, M., Gallini, C.A., Bohlooly-Y, M., Glickman, J.N., and Garrett, W.S. (2013). The microbial metabolites, short chain fatty acids, regulate colonic Treg cell homeostasis. Science *341*, 10.1126/science.1241165. https://doi.org/10.1126/science.1241165.

Stare, F.J. (1963). Overnutrition. Am J Public Health Nations Health *53*, 1795-1802. .

Stearns, S.C. (1989). Trade-Offs in Life-History Evolution. Functional Ecology *3*, 259-268. https://doi.org/10.2307/2389364.

Thaiss, C.A., Zeevi, D., Levy, M., Zilberman-Schapira, G., Suez, J., Tengeler, A.C., Abramson, L., Katz, M.N., Korem, T., Zmora, N., et al. (2014). Transkingdom Control of Microbiota Diurnal Oscillations Promotes Metabolic Homeostasis. Cell *159*, 514-529. https://doi.org/10.1016/j.cell.2014.09.048.

Thaiss, C.A., Levy, M., Korem, T., Dohnalová, L., Shapiro, H., Jaitin, D.A., David, E., Winter, D.R., Gury-BenAri, M., Tatirovsky, E., et al. (2016). Microbiota Diurnal Rhythmicity Programs Host Transcriptome Oscillations. Cell *167*, 1495-1510.e12. https://doi.org/10.1016/j.cell.2016.11.003.

Turnbaugh, P.J., Ley, R.E., Mahowald, M.A., Magrini, V., Mardis, E.R., and Gordon, J.I. (2006). An obesity-associated gut microbiome with increased capacity for energy harvest. Nature *444*, 1027-1031. https://doi.org/10.1038/nature05414.

Ueno, T., Tremblay, J., Kunes, J., Zicha, J., Dobesova, Z., Pausova, Z., Deng, A.Y., Sun, Y.-L., Jacob, H.J., and Hamet, P. (2004). Rat model of familial combined hyperlipidemia as a result of comparative mapping. Physiol Genomics *17*, 38-47. https://doi.org/10.1152/physiolgenomics.00043.2003.

Võikar, V., Kõks, S., Vasar, E., and Rauvala, H. (2001). Strain and gender differences in the behavior of mouse lines commonly used in transgenic studies. Physiology & Behavior *72*, 271-281. https://doi.org/10.1016/S0031-9384(00)00405-4.

Walton, J.C., Bumgarner, J.R., and Nelson, R.J. (2022). Sex Differences in Circadian Rhythms. Cold Spring Harb Perspect Biol *14*, a039107. https://doi.org/10.1101/cshperspect.a039107.

Wang, G.-Z., Hickey, S.L., Shi, L., Huang, H.-C., Nakashe, P., Koike, N., Tu, B.P., Takahashi, J.S., and Konopka, G. (2015). Cycling Transcriptional Networks Optimize Energy Utilization on a Genome Scale. Cell Reports *13*, 1868-1880. https://doi.org/10.1016/j.celrep.2015.10.043.

Wang, Y., Kuang, Z., Yu, X., Ruhn, K.A., Kubo, M., and Hooper, L.V. (2017). The intestinal microbiota regulates body composition through NFIL3 and the circadian clock. Science *357*, 912-916. https://doi.org/10.1126/science.aan0677.

Weger, B.D., Gobet, C., Yeung, J., Martin, E., Jimenez, S., Betrisey, B., Foata, F., Berger, B., Balvay, A., Foussier, A., et al. (2019). The Mouse Microbiome Is Required for Sex-Specific Diurnal Rhythms of Gene Expression and Metabolism. Cell Metabolism *29*, 362-382.e8. https://doi.org/10.1016/j.cmet.2018.09.023.

West-Eberhard, M.J. (1989). Phenotypic Plasticity and the Origins of Diversity. Annual Review of Ecology and Systematics *20*, 249-278. .

Yatsunenko, T., Rey, F.E., Manary, M.J., Trehan, I., Dominguez-Bello, M.G., Contreras, M., Magris, M., Hidalgo, G., Baldassano, R.N., Anokhin, A.P., et al. (2012). Human gut microbiome viewed across age and geography. Nature *486*, 222-227. https://doi.org/10.1038/nature11053.

Zarrinpar, A., Chaix, A., Yooseph, S., and Panda, S. (2014). Diet and feeding pattern affect the diurnal dynamics of the gut microbiome. Cell Metabolism *20*, 1006-1017. .

Zarrinpar, A., Chaix, A., and Panda, S. (2016). Daily Eating Patterns and Their Impact on Health and Disease. Trends in Endocrinology & Metabolism *27*, 69-83. https://doi.org/10.1016/j.tem.2015.11.007.

Zarrinpar, A., Chaix, A., Xu, Z.Z., Chang, M.W., Marotz, C.A., Saghatelian, A., Knight, R., and Panda, S. (2018). Antibiotic-induced microbiome depletion alters metabolic homeostasis by affecting gut signaling and colonic metabolism. Nat Commun *9*, 2872. https://doi.org/10.1038/s41467-018-05336-9.

Zeng, X., Xing, X., Gupta, M., Keber, F.C., Lopez, J.G., Lee, Y.-C.J., Roichman, A., Wang, L., Neinast, M.D., Donia, M.S., et al. (2022). Gut bacterial nutrient preferences quantified in vivo. Cell *185*, 3441-3456.e19. https://doi.org/10.1016/j.cell.2022.07.020.

Zheng, D., Ratiner, K., and Elinav, E. (2020). Circadian Influences of Diet on the Microbiome and Immunity. Trends Immunol *41*, 512-530. https://doi.org/10.1016/j.it.2020.04.005.

# Materials and Methods

## EXPERIMENTAL MODEL AND SUBJECT DETAILS

### Animals and tissue collection

All experiments were approved by the University of Pittsburgh and Magee-Womens Research Institute Institutional Animal Care and Use Committee and performed in accordance with National Institutes of Health Animal Care and Use Guidelines. C57Bl/6N mice from Taconic Biosciences (C57Bl/6NTac) and C57Bl/6 from Jackson Laboratories (C57Bl/6Jax) arrived at the animal facility aged three weeks. Mice were allowed to acclimate to animal facilities until aged 10 weeks prior to experimentation. All mice were maintained on a 12-hour light/dark cycle (lights on: 0600, Zeitgeber time (ZT) 0; lights off: 1800, ZT 12). An Onset HOBO MX2202 Wireless Temperature/Light Data Logger (HOBO Data Loggers, Wilmington, NC) was used to confirm stability of light: dark photoperiod. *Ad libitum* access was provided to water and a chow diet (PicoLab Mouse Diet 20, St. Louis, MO; 23.2% protein, 55.2% carbohydrate, 21.6% fat). For circadian collections, three mice from each condition from separate cages were euthanized and whole blood, ileum, cecum, and brain samples were during a 24h period for each of the 6 timepoints on the Zeitgeber time scale (ZT0, ZT4, ZT8, ZT12, ZT16, ZT20). Due to limitations in after-hours access to gnotobiotic facilities, circadian collections of germ-free mice occurred at 4 timepoints (ZT4, ZT8, ZT12, ZT16). Ileum, cecum, and brain samples were rapidly frozen on dry ice and stored at -80C until further processing.

## METHOD DETAILS

### Cecal luminal content DNA extraction and 16S rRNA marker gene sequencing

The MagAttract PowerMicrobiome DNA/RNA Kit (Qiagen) extracted genomic DNA from fifty milligram of cecal luminal contents, using bead-beating on a TissueLyser II (Qiagen), according to

the manufacturer's instructions. 16S libraries were generated using a two-step PCR protocol. Amplicon PCR was performed as follows for amplification of the 16s rRNA V3-V4 region from cecal luminal contents: initial denaturation at 95°C for 3 minutes, following by 25-cyles 95°C for 30 seconds, 55°C for 30 seconds, 72°C for 30 seconds, and a final extension at 72°C for 5 minutes. Resultant 16S V3-V4 amplicons were then purified using AMPure XP beads at a 0.8 ratio of beads to amplicon volume. Illumina Nextera XT Index Primer 1 (N7xx) and Nextera XT Index Primer 2 (S5xx) were used as index primers. Index PCR was performed as follows for amplification of the 16s rRNA V3-V4 region from cecal luminal contents: initial denaturation at 95°C for 3 minutes, following by 8-cyles 95°C for 30 seconds, 55°C for 30 seconds, 72°C for 30 seconds, and a final extension at 72°C for 5 minutes. Results indexed libraries were cleaned up using AMPure XP beads at a 0.8 ratio of beads to indexed library. The concentration of indexed libraries was quantified using Qubit and library fragment size was quantified using an Agilent Tapestation 4200 with D5000 ScreenTapes. Libraries were normalized, pooled, and a paired-end sequencing of pooled libraries was done on an Illumina iSeq 100 System using 2x150bp run geometry in our laboratory.

**Ileum RNA extraction and preparation for RNA-seq**

Frozen tissue samples were homogenized in TRIzol Reagent (Life Technologies #15596026) using a MiltenyiBiotec gentleMACS Octo Dissociator for 30s. RNA was isolated with Qiagen RNeasy Mini Kits according to the manufacturer's instructions. RNA integrity was quantified on an Agilent Tapestation 4200 using TapeStation RNA ScreenTapes. All samples had an RIN score above 8. Sequencing libraries were prepared using Illumina Stranded mRNA prep, Ligation kits with IDT for Illumina RNA UD Indexes Set A, Ligation index adapters. The concentration of indexed libraries was quantified using Qubit and library fragment size was quantified using an Agilent Tapestation 4200 with D5000 ScreenTapes. Sequencing was performed on an Illumina NextSeq 2000 using P3 flow

cells and 2x100 paired end-run geometry at the Health Sciences Sequencing Core at Children's Hospital of Pittsburgh. Sequencing was repeated twice on the same library pool to achieve sufficient resolution and minimize batch effects, producing a yield of an average of 30 – 60 million reads per sample.

**Quantification of 3NP-Short Chain Fatty Acids**

Cecal samples were homogenized with 50% aqueous acetonitrile at a ratio of 1:15 vol: wt. 5µg/mL Deuterated internal standards: (D2)-formate, (D4)-acetate, (D5)-butyrate, (D6)-propionate, (D2)-valerate and (D4)-hexanoate (CDN Isotopes, Quebec, Canada) were added. Samples were homogenized using a FastPrep-24 system (MP-Bio), with Matrix D at 60hz for 30 seconds, before being cleared of protein by centrifugation at 16,000xg. Plasma samples were cleared of protein using 4x volumes ice cold 1:1 MeOH: EtOH with vortexing, followed by centrifugation at 16,000xg. 60µL cleared supernatants were collected and derivatized using 3-nitrophenylhydrazine. Each sample was mixed with 20 µL of 200 mM 3-nitrophenylhydrazine in 50% aqueous acetonitrile and 20 µL of 120 mM N-(3-dimethylaminopropyl)-N0-ethylcarbodiimide -6% pyridine solution in 50% aqueous acetonitrile. The mixture reacted at 60□C for 40 minutes and the reaction was stopped with 0.45 mL of 50% acetonitrile. Derivatized samples were injected (50 µL) via a Thermo Vanquish UHPLC and separated over a reversed phase Phenomenex Kinetex 150mm x 2.1mm 1.7µM particle C18 maintained at 55°C. For the 20-minute LC gradient, the mobile phase consisted of the following: solvent A (water / 0.1% FA) and solvent B (ACN / 0.1% FA). The gradient was the following: 0-2min 15% B, increase to 60%B over 10 minutes, continue increasing to 100%B over 1 minute, hold at 100%B for 3 minutes, reequillibrate at 15%B for 4 minutes. The Thermo IDX tribrid mass spectrometer was operated in both positive ion mode, scanning in ddMS2 mode (2 µscans) from 75 to 1000 m/z at 120,000 resolutions with an AGC target of 2e5 for full scan, 2e4 for ms2

scans using HCD fragmentation at stepped 15,35,50 collision energies. Source ionization setting was 3.0kV spray voltage respectively for positive mode. Source gas parameters were 45 sheath gas, 12 auxiliary gas at 320°C, and 3 sweep gas. Calibration was performed prior to analysis using the PierceTM FlexMix Ion Calibration Solutions (Thermo Fisher Scientific). Integrated peak areas were then extracted manually using Quan Browser (Thermo Fisher Xcalibur ver. 2.7). SCFA are reported as the area ratio of SCFA to the internal standard (Han et al., 2015).

## QUANTIFICATION AND STATISTICAL ANALYSIS

### Processing and analysis of 16S rRNA marker gene sequencing data

The sequences were demultiplexed on the BaseSpace Sequence Hub using the bcl2fastq2 conversion software version 2.2.0. Quality control on the resulting demultiplexed forward fastq files were performed using DADA2 denoise-single function with trimming 33bp of the primer sequence. A Naive Bayes feature classifier was trained using SILVA reference sequences with the q2-feature-classifier for taxonomic analysis. The average count per sample was 24,717, with maximum count per sample at 39,048 and minimum count per sample at 10,161. MicrobiomeAnalyst was used for statistical and meta-analysis of the data. Data filtering was set to include features where 20% of its values contain a minimum of four counts. In addition, features that exhibit low variance across treatment conditions are unlikely to be associated with treatment conditions, and therefore variance was measured by interquartile range and removed at 10%. Data were normalized by using trimmed mean of M-values. For quality control purposes, water and processed blank samples were sequenced and analyzed through the bioinformatics pipeline. Taxa identified as cyanobacteria or 'unclassified' to the phylum level were removed. Oscillation of microbiota abundance and period of oscillation were detected using Cosinor analysis using the R package DiscoRhythm (Carlucci et al., 2019). Taxa with $p < 0.05$ over a 24-h oscillation period are reported.

## Processing and analysis of bulk RNA-seq data

Concatenated FASTQ files generated from Illumina were used as input to kallisto, a program that pseudoaligns high-throughput sequencing reads to the *Mus musculus* reference transcriptome (version 38) and quantifies transcript expression. We used 60 bootstrap samples to ensure accurate transcript quantification. Gene isoforms were collapsed to gene symbols using the Bioconductor package tximport (version 3.4). Genes were filtered to counts per million >1 in at least three samples. The filtered gene list was normalized using trimmed mean of M-values in edgeR. Oscillation of microbiota abundance and period of oscillation were detected using Cosinor analysis using the R package DiscoRhythm (Carlucci et al., 2019). Transcripts with $p < 0.05$ over a 24-h oscillation period are reported. Over-representation analysis of Gene Ontology: Biological Process terms to identify enriched molecular pathways/processes in both the top enriched and top rhythmic gene lists was performed with clusterProfiler and PantherDB.

## Analysis of targeted metabolomics data

Oscillation of absolute or relative metabolite abundance and period of oscillation were detected using Cosinor analysis using the R package DiscoRhythm (Carlucci et al., 2019). Metabolites with $p < 0.05$ over a 24-h oscillation period are reported.

## Quantification and statistical analysis

Statistical information including sample size, mean, and statistical significance values are shown in the text or the figure legends. A variety of statistical analyses were applied, each one specifically appropriate for the data and hypothesis, using the R statistical environment. For standard metabolic endpoints, analysis of variance (ANOVA) testing with repeated-measures corrections and Tukey post-hoc tests were used, with significance at an adjusted $p < 0.05$. Processing of RNA-Seq data was conducted using standardized and published protocols. Cytobank and Astrolabe Diagnostics were used for analysis of CyTOF data using default settings. GraphPad Prism and Adobe Illustrator were used for generating figures. No custom script was used to analyze RNA sequencing or cytometric data.

**Statistical analysis of data**

Number of samples used per time point and condition are described under ‘Animals and tissue collection’ section and in the caption of each associated figure along with the statistical method used for analysis. All analyses were performed in python version 3.6.12 (Python Software, 2020) or R version 4.1.0 (R Core Team, 2021).

## FIGURES

**Figure 1.**

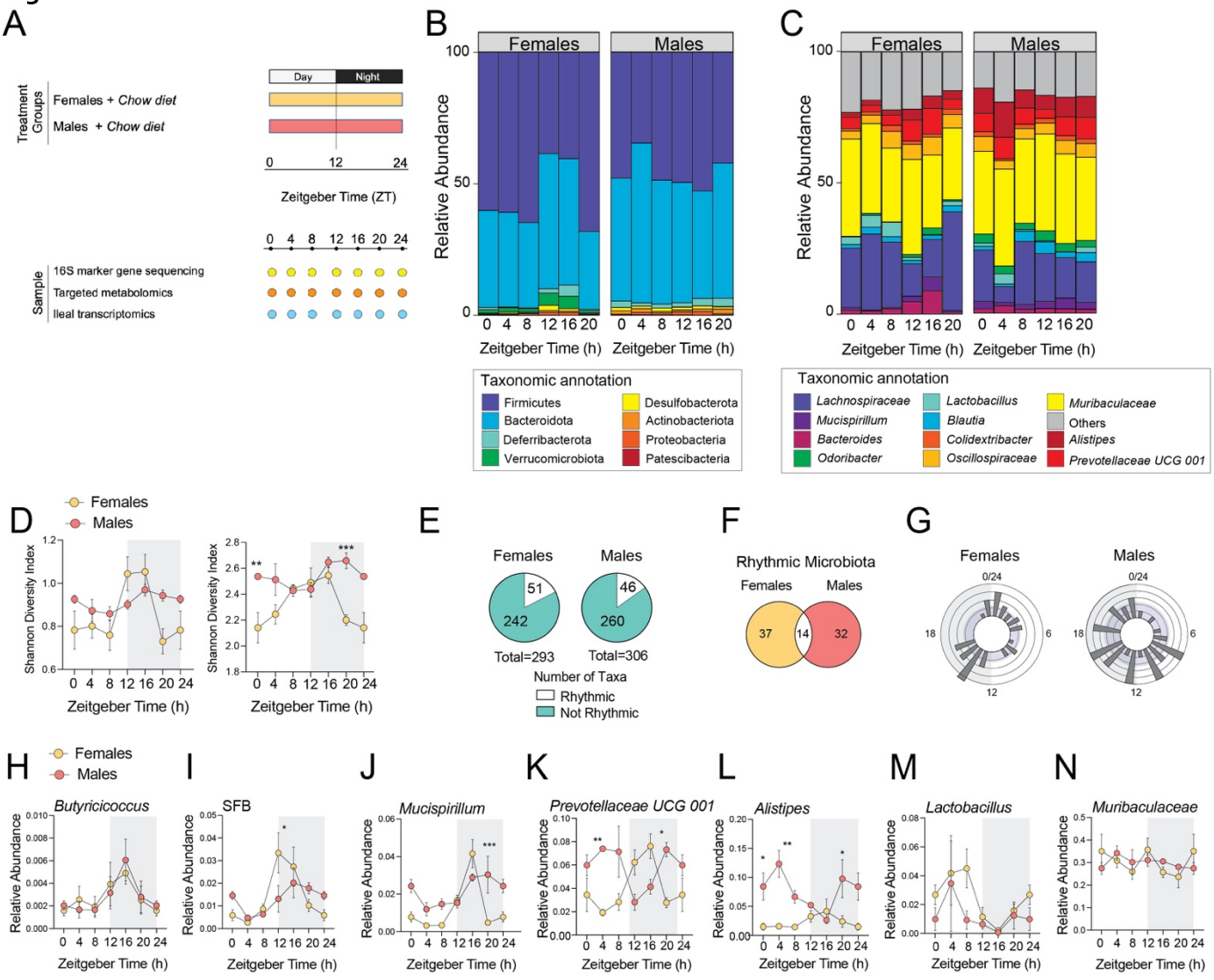


**Figure 1.** Cecal microbiota composition is time-of-day dependent and differs by sex.

A) Schematic representation of study design and sample collections.

B) Relative abundance of top eight phyla by time points for each condition.

C) Relative abundance of top twelve genera by time points for each condition.

D) Measures of alpha-diversity (Shannon Diversity Index) across time in males and females at phyla (top) and genus (bottom) level. *Top panel*, phylum-level alpha diversity differed by time-of-day in males and females (time*sex interaction, $F_{6,\ 23}$ = 3.260, $p$ = 0.0181). *Bottom panel*, genus-level alpha diversity differed by time-of-day in males and females (time*sex interaction, $F_{6,\ 27}$ = 4.373, $p$ =0.0033).

E) Sex differences in non-rhythmic and rhythmic microbiota detected in the cecum using cosinor analysis.

F) Rose plot showing sex differences in acrophase distribution of microbiota in the cecum of adult females (left) and males (right).

G) Venn diagram depicting sex-specific and shared rhythmic cecal microbiota.

H) Relative abundance of cecal *Butyricicoccus* shows similar rhythmicity in males and females with peak abundance around ZT16 (main effect of time, $F_{6, 23} = 3.098$, $p = 0.0226$)

I) Relative abundance of cecal Segmented Filamentous Bacteria shows sex-specific rhythmicity (time*sex, $F_{6, 27} = 2.850$, $p = 0.0279$), with peak abundance occurring in females prior to males (ZT12 vs. ZT16, respectively).

J) Relative abundance of cecal *Mucispirillum* shows sex-specific rhythmicity (time*sex, $F_{6, 27} = 4.850$, $p = 0.0018$).

K) Relative abundance of cecal *Prevotellaceae UCG 001* shows sex-specific rhythmicity (time*sex, $F_{6, 27} = 6.414$, $p = 0.0004$).

L) Relative abundance of cecal *Alistipes* shows sex-specific rhythmicity (time*sex, $F_{6, 27} = 3.190$, $p = 0.0169$), with a male-specific increase during the behavioral inactive phase but not females.'

M) Relative abundance of cecal *Lactobacillus* shows sex-specific abundance regardless of time-of-day (main effect of sex, $F_{1, 27} = 4.762$, $p = 0.0380$), with females showing higher overall abundance of this taxa.

N) Relative abundance of cecal Muribaculaceae (formerly S24-7) is stable across time-of-day in males and females (all *p's* > 0.05).

Three murine-pathogen free C57Bl/6NTac females and males were used for each condition, for a total of 18 males and 18 females. Acrophases were calculated by cosinor analysis (period = 24 h). Threshold for the cosinor test was set to $p < 0.05$. Data is represented as mean ± SEM. *$p < 0.05$, ** $p < 0.01$, *** $p < 0.001$ following Bonferroni correction for multiple testing.

## Figure 2.

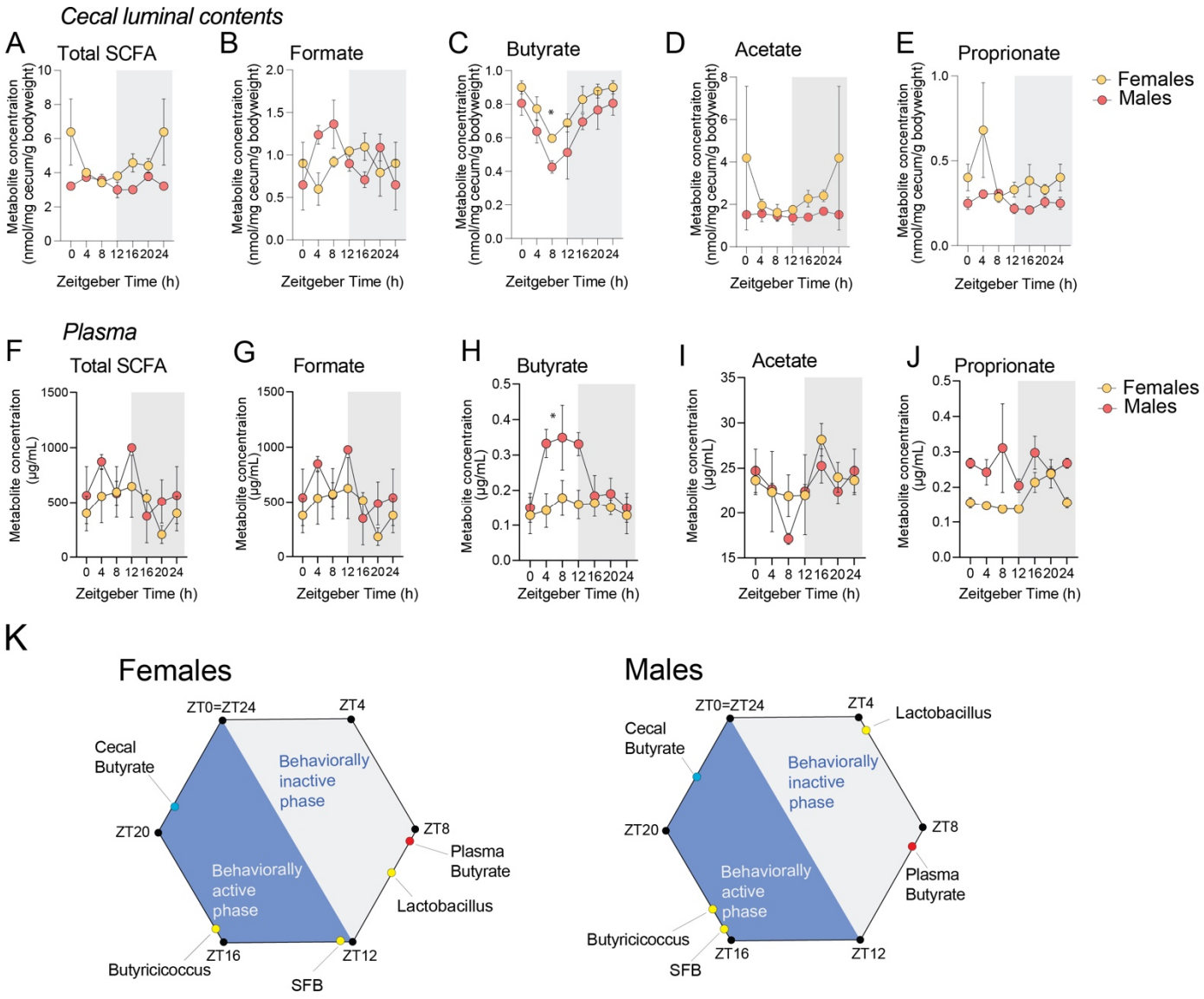


**Figure 2.** Local and systemic availability of microbial metabolite varies by time-of-day and differs by sex.

A) Availability of total SCFA in cecal lumen is similar across time-of-day in males and females (all *p's* > 0.05).

B) Availability of formate in cecal lumen is similar across time-of-day in males and females (all *p's* > 0.05).

C) Availability of butyrate in cecal lumen shows sex-specific rhythmicity (main effect of sex, $F_{1,4} = 8.90$, $p = 0.0435$; main effect of time, $F_{6,24} = 6.795$, $p = 0.0003$) characterized by a transient sex difference in butyrate availability ZT8 that later disappears during the behavioral active phase.

D) Availability of acetate in cecal lumen is similar across time-of-day in males and females (all *p's* > 0.05).

E) Availability of propionate in cecal lumen is similar across time-of-day in males and females (all *p's* > 0.05).

F) Availability of total SCFA in plasma is similar across time-of-day in males and females (all *p's* > 0.05).

G) Availability of formate in plasma is similar across time-of-day in males and females (all *p's* > 0.05).

I) Availability of butyrate in plasma shows sex-specific rhythmicity, with males showing greater availability than females during the behavioral inactive phase (ZT4, $t_{27}$ = 1.935, $p$ = 0.0636).

I) Availability of acetate in plasma differs between males and females (main effect of sex, $F_{1,4}$ = 28.97, $p$ = 0.0058, with males showing greater availability than females.

J) Availability of propionate in plasma is similar across time-of-day in males and females (all *p's* > 0.05).

K) Comparison of acrophases of cecal microbiota abundance and cecal and plasma short-chain fatty acid concentration in females (left) and males (right). Light and dark phases are shaded in white and blue, respectively.

Three murine-pathogen free C57Bl/6NTac females and males were used for each condition, for a total of 18 males and 18 females. Acrophases were calculated by cosinor analysis (period = 24 h). Data is represented as mean ±SEM.

Figure 3.

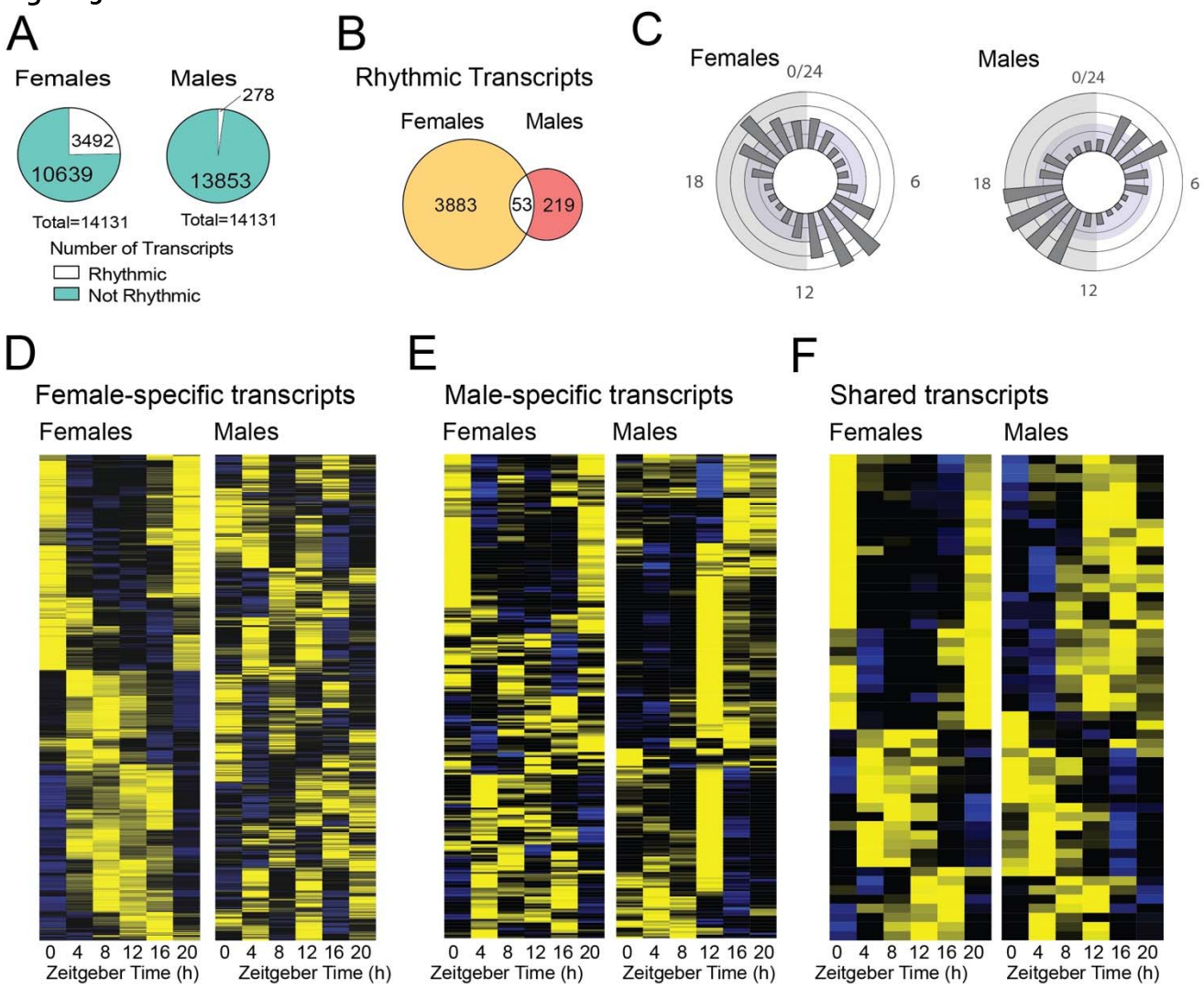


**Figure 3.** Transcriptional landscape of the adult ileum is time-of-day dependent and differs by sex.

A) Sex differences in non-rhythmic and rhythmic transcripts detected in the ileum using cosinor analysis.

B) Venn diagram depicting sex-specific and shared rhythmic transcripts.

C) Rose plot showing sex differences in acrophase distribution of genes in the adult ileum of females (left) and males (right).

D) Heatmap showing expression levels of 3492 genes that have circadian cycling in the adult female ileum, as detected by cosinor analysis.

E) Heatmap showing expression levels of 278 genes that have circadian cycling in the adult male ileum, as detected by cosinor analysis.

F) Heatmap showing expression levels of 53 genes that have circadian cycling in the adult ileum of both sexes, as detected by cosinor analysis.

Three murine-pathogen free C57Bl/6NTac females and males were used for each condition, for a total of 18 males and 18 females. Acrophases were calculated by cosinor analysis (period = 24 h). Threshold for the cosinor test was set to $p < 0.05$.

**Figure 4.**

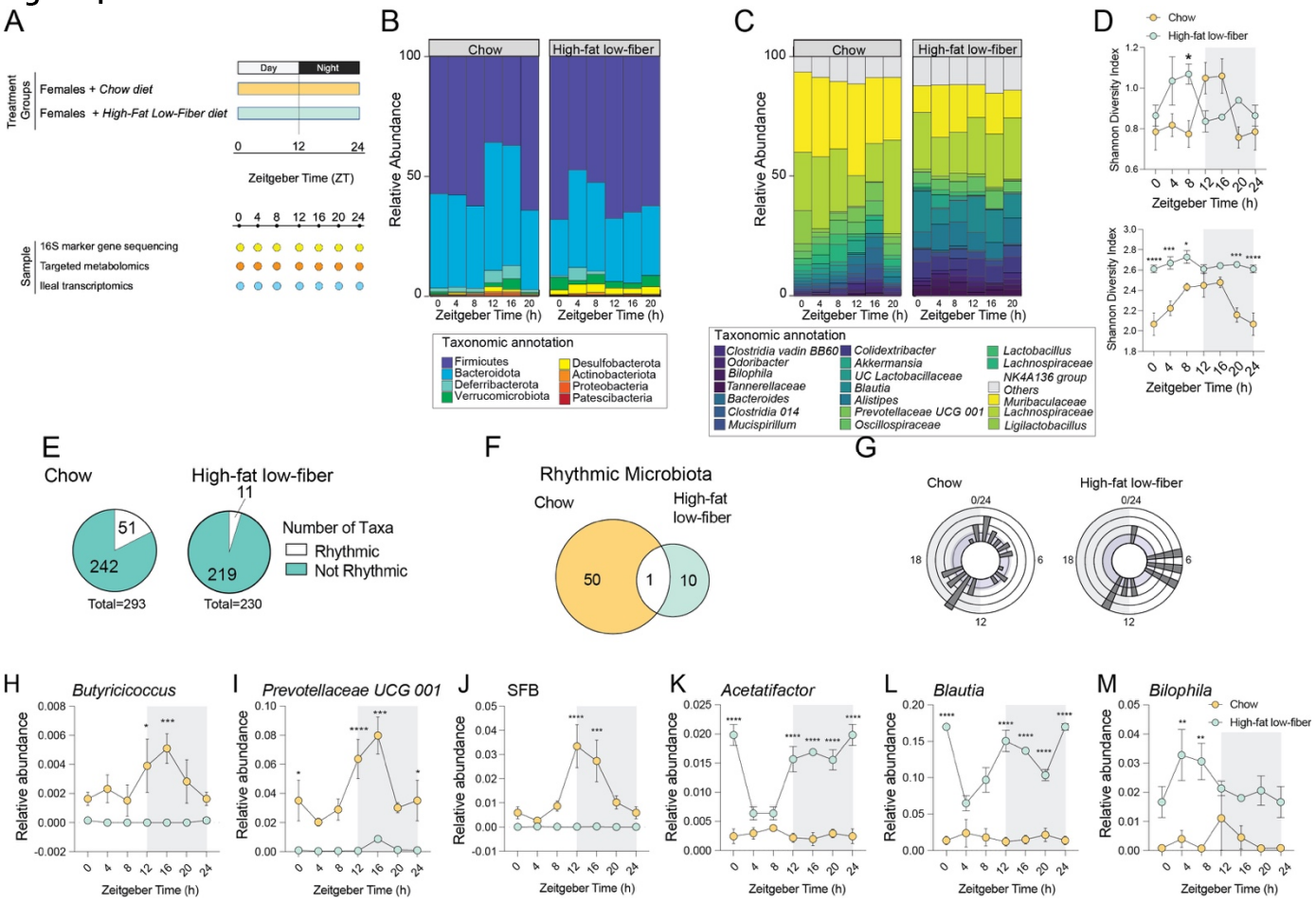


**Figure 4. Consumption of a high-fat low-fiber diet drives acquisition of new diurnal rhythms in the cecal microbiota of females.**

A) Schematic representation of study design and sample collections.

B) Relative abundance of top eight phyla by time points for each condition.

C) Relative abundance of top twenty genera by time points for each condition.

D) Measures of alpha-diversity (Shannon Diversity Index) across time in females consuming a chow or high-fat low-fiber diet at phyla (top) and genus (bottom) level. *Top panel*, phylum-level alpha diversity differed by time-of-day and diet (time*sex interaction, $F_{6,\ 23} = 4.245$, $p = 0.0051$). *Bottom panel*, genus-level alpha diversity differed by time-of-day and diet (time*sex interaction, $F_{6,\ 27} = 3.289$, $p = 0.017$).

E) Female-specific diet differences in non-rhythmic and rhythmic microbiota detected in the cecum using cosinor analysis.

G) Venn diagram depicting diet-specific and shared rhythmic cecal microbiota.

F) Rose plot showing sex differences in acrophase distribution of microbiota in the cecum of females consuming either chow (left) or high-fat low-fiber diet (right).

H) Relative abundance of cecal *Butyricicoccus* shows diet-specific rhythmicity (main effect of diet, $F_{1, 4}$ = 20.41, $p$ = 0.011)

I) Relative abundance of cecal *Prevotellaceae UCG 001* shows diet-specific rhythmicity (main effect of diet, $F_{1, 4}$ = 72.92, $p$ = 0.001).

J) Relative abundance of cecal Segmented Filamentous Bacteria shows diet-specific rhythmicity (time*diet, $F_{6, 26}$ = 4.58, $p$ = 0.0027).

K) Relative abundance of cecal *Acetatifactor* shows diet-specific increase in females consuming a high-fat low-fiber diet across the day (time*diet, $F_{6, 22}$ = 11.50, $p$ <0.0001).

L) Relative abundance of cecal *Blautia* shows diet-specific increase in females consuming a high-fat low-fiber diet across the day (time*diet, $F_{6, 26}$ = 8.88, $p$ < 0.0001).

M) Relative abundance of cecal *Bilophila* shows diet-specific increase in females consuming a high-fat low-fiber diet (main effect of diet, $F_{1, 4}$ = 21.29, $p$ = 0.009).

Three murine-pathogen free C57Bl/6NTac females consuming either a chow or high-fat and low-fiber diet were used for each condition, for a total of 18 males and 18 females. Acrophases were calculated by cosinor analysis (period = 24 h). Threshold for the cosinor test was set to $p < 0.05$. Data is represented as mean ± SEM. *$p$ < 0.05, ** $p$ < 0.01, *** $p$ < 0.001 following Bonferroni correction for multiple testing.

Figure 5.

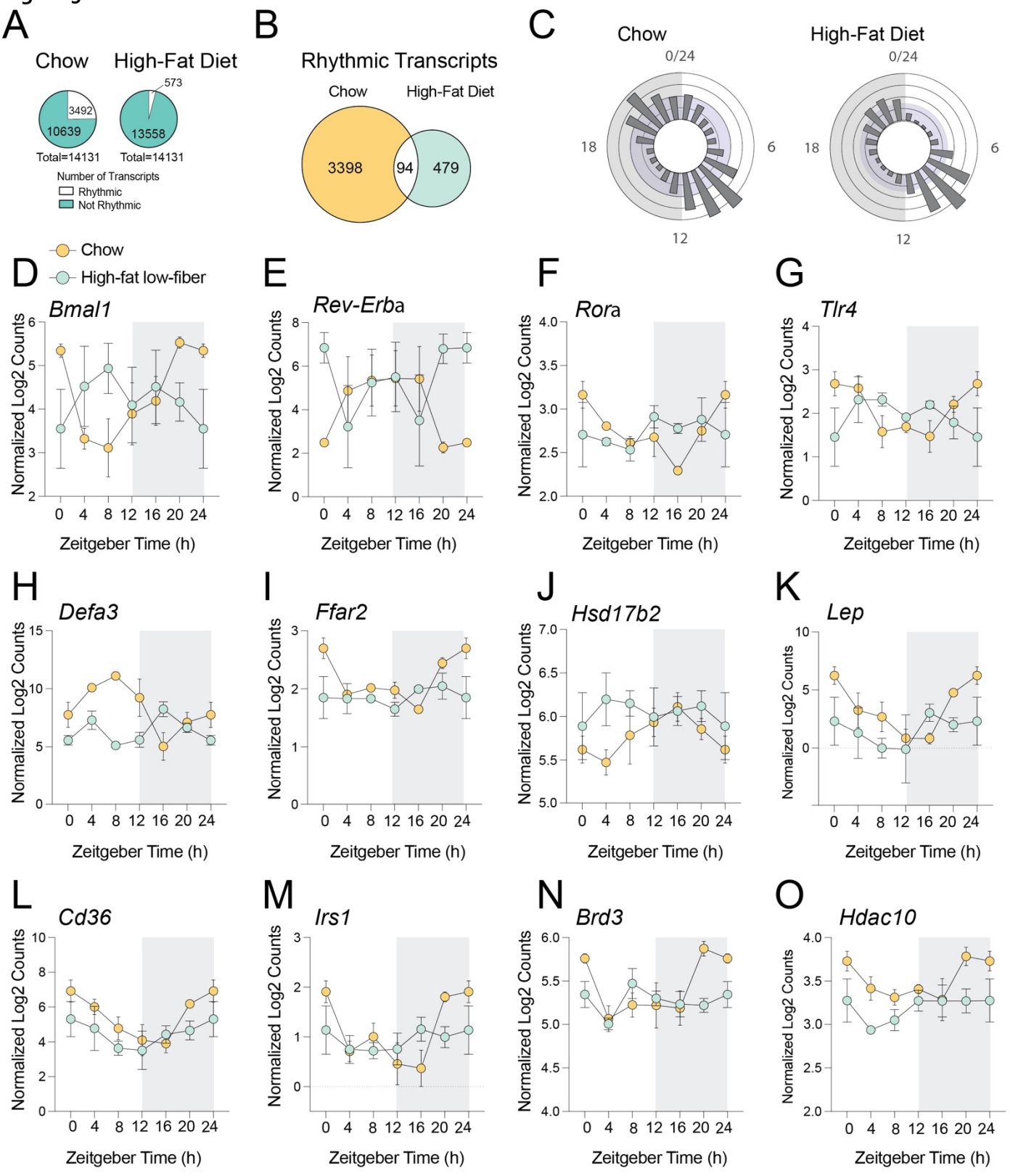


Figure 5. Diet-mediated disruption of genes involved in the molecular clock, metabolism, and histone post-translational modification.

A) Female-specific diet differences in non-rhythmic and rhythmic transcripts detected in the ileum using cosinor analysis.

B) Venn diagram depicting diet-specific and shared rhythmic transcripts.

C) Rose plot showing sex differences in acrophase distribution of transcripts in females consuming either chow (left) or high-fat low-fiber diet (right).

(D-F) Expression of genes involved in the mammalian molecular clock in the ileum is disrupted by consumption of a high-fat low-fiber diet.

(G-H) Expression of genes involved in innate immunity in the ileum is disrupted by consumption of a high-fat low-fiber diet.

(I-M) Expression of genes involved in metabolic function in the ileum is disrupted by consumption of a high-fat low-fiber diet.

(N-O) Expression of genes involved in histone post-translational modifications in the ileum is disrupted by consumption of a high-fat low-fiber diet.

Three murine-pathogen free C57Bl/6NTac females consuming either a chow or high-fat and low-fiber diet were used for each condition, for a total of 18 males and 18 females. Threshold for the cosinor test was set to $p < 0.05$. Data is represented as mean ± SEM.

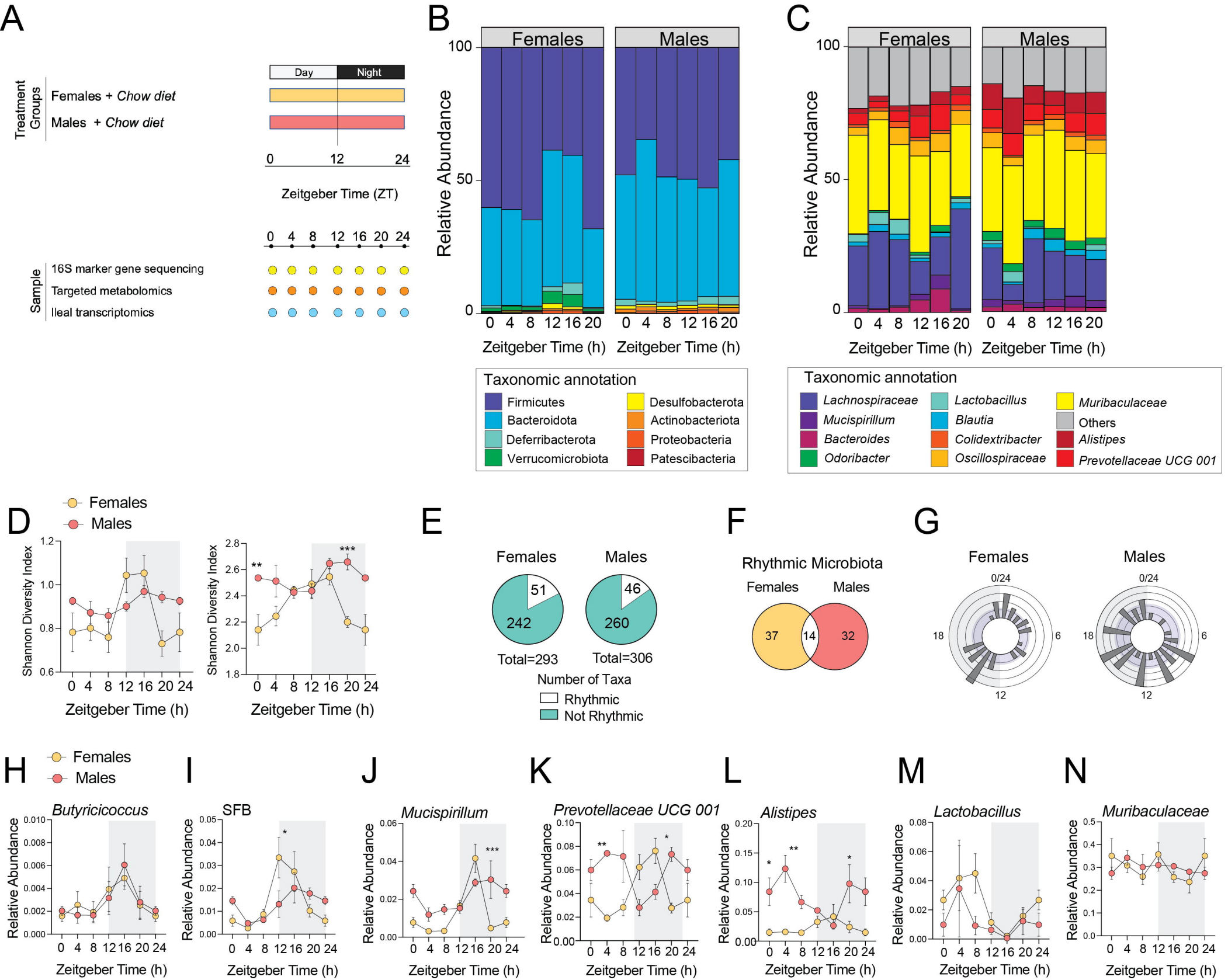
A
Treatment Groups
Females + Chow diet
Males + Chow diet
Day
Night
0
12
24
Zeitgeber Time (ZT)
0 4 8 12 16 20 24
Sample
16S marker gene sequencing
Targeted metabolomics
Ileal transcriptomics
B
Females
Males
Relative Abundance
100
50
0
0 4 8 12 16 20
Zeitgeber Time (h)
Taxonomic annotation
Firmicutes
Bacteroidota
Deferribacterota
Verrucomicrobiota
Desulfobacterota
Actinobacteriota
Proteobacteria
Patescibacteria
C
Females
Males
Relative Abundance
Zeitgeber Time (h)
Taxonomic annotation
Lachnospiraceae
Mucispirillum
Bacteroides
Odoribacter
Lactobacillus
Blautia
Colidextribacter
Oscillospiraceae
Muribaculaceae
Others
Alistipes
Prevotellaceae UCG 001
D
Females
Males
Shannon Diversity Index
Zeitgeber Time (h)
E
Females
Males
51
242
46
260
Total=293
Total=306
Number of Taxa
Rhythmic
Not Rhythmic
F
Rhythmic Microbiota
Females
Males
37
14
32
G
Females
Males
0/24
6
12
18
H
Butyricicoccus
I
SFB
J
Mucispirillum
K
Prevotellaceae UCG 001
L
Alistipes
M
Lactobacillus
N
Muribaculaceae
Relative Abundance
Zeitgeber Time (h)

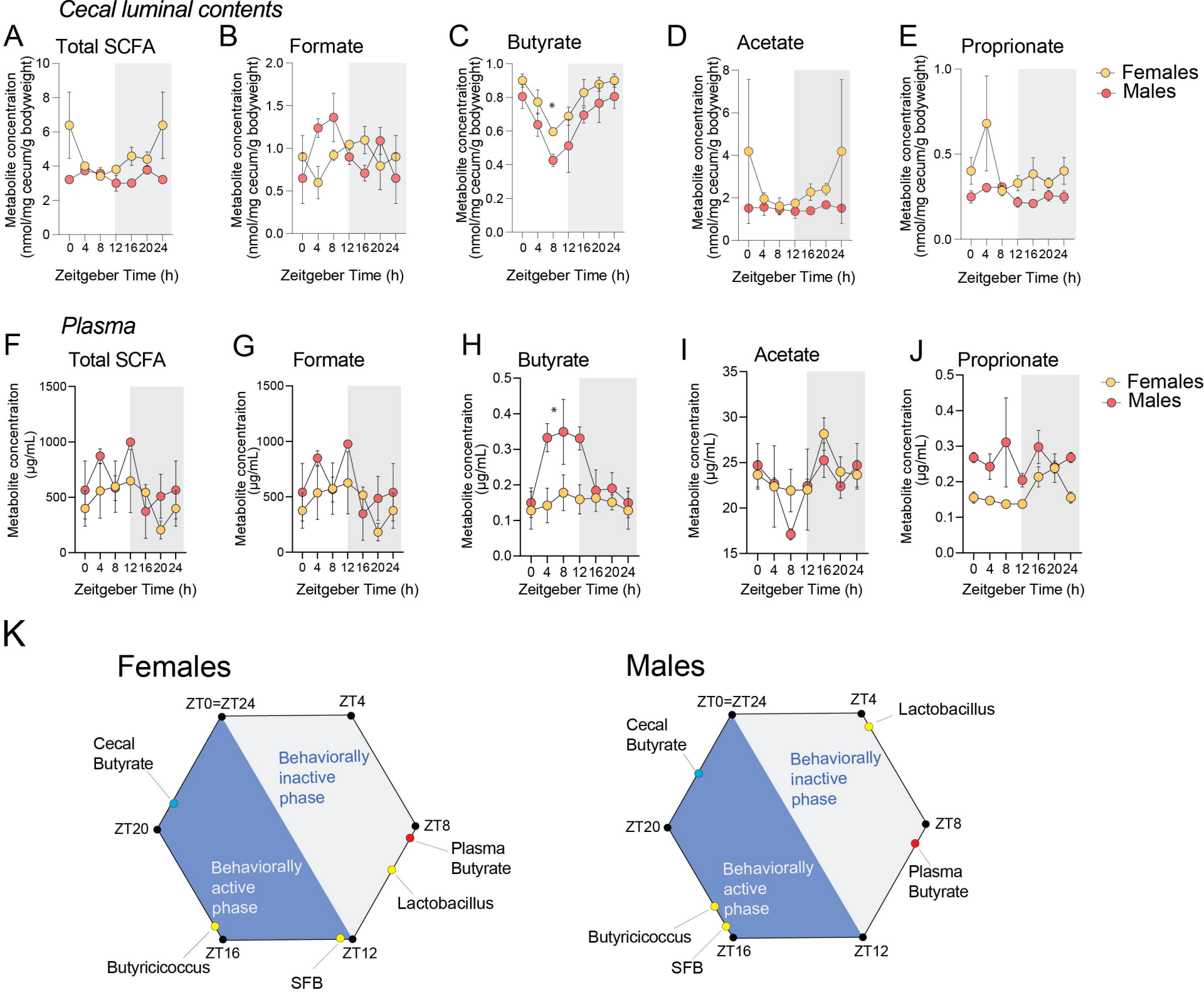
Cecal luminal contents
A
Total SCFA
B
Formate
C
Butyrate
D
Acetate
E
Proprionate
Metabolite concentraiton (nmol/mg cecum/g bodyweight)
Zeitgeber Time (h)
Females
Males
Plasma
F
Total SCFA
G
Formate
H
Butyrate
I
Acetate
J
Proprionate
Metabolite concentraiton (µg/mL)
K
Females
ZT0=ZT24
ZT4
ZT8
ZT12
ZT16
ZT20
Cecal Butyrate
Plasma Butyrate
Lactobacillus
Butyricicoccus
SFB
Behaviorally inactive phase
Behaviorally active phase
Males

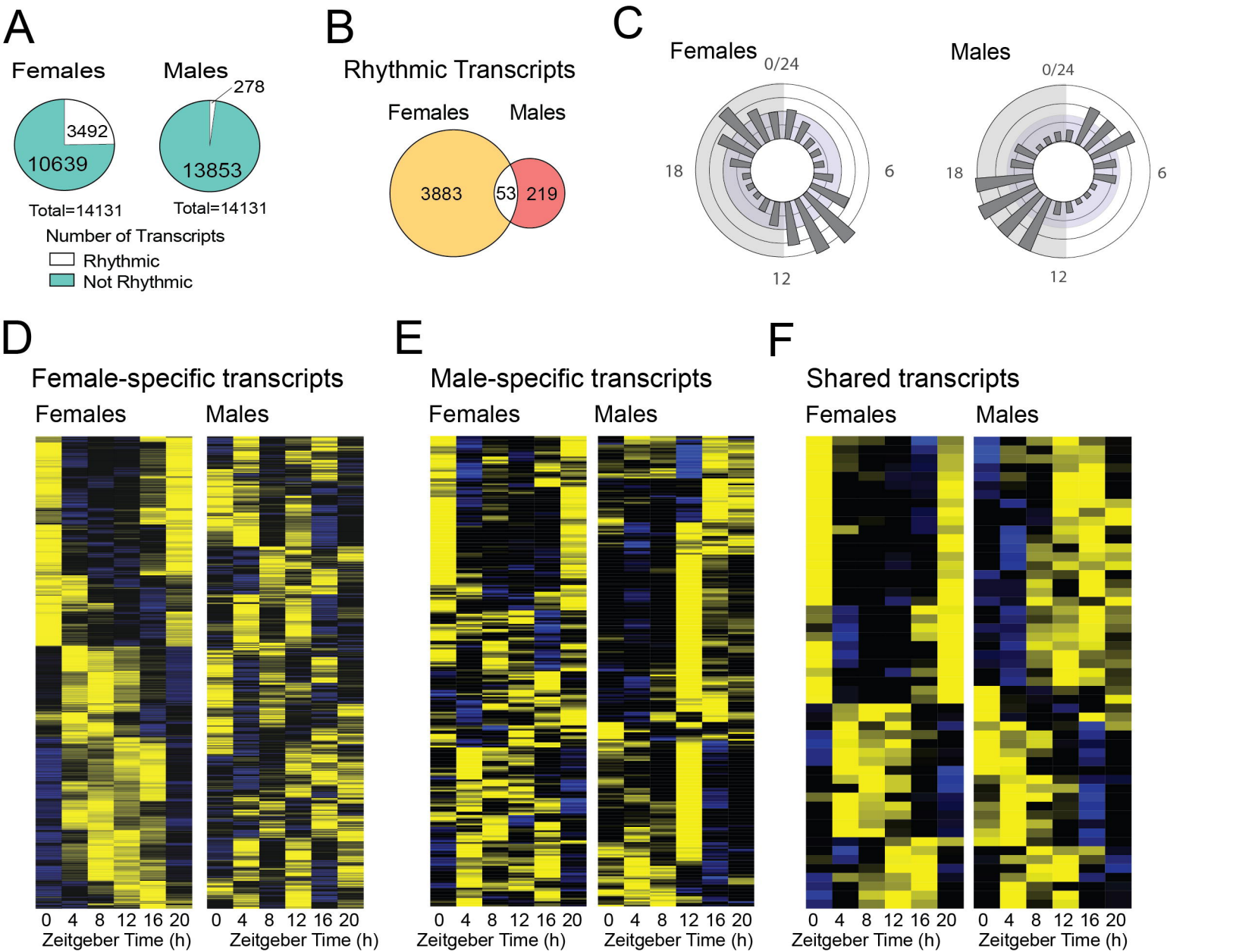
A
Females
Males
3492
10639
278
13853
Total=14131
Total=14131
Number of Transcripts
Rhythmic
Not Rhythmic
B
Rhythmic Transcripts
Females
Males
3883
53
219
C
Females
Males
0/24
6
12
18
D
Female-specific transcripts
Females
Males
E
Male-specific transcripts
Females
Males
F
Shared transcripts
Females
Males
0 4 8 12 16 20
Zeitgeber Time (h)

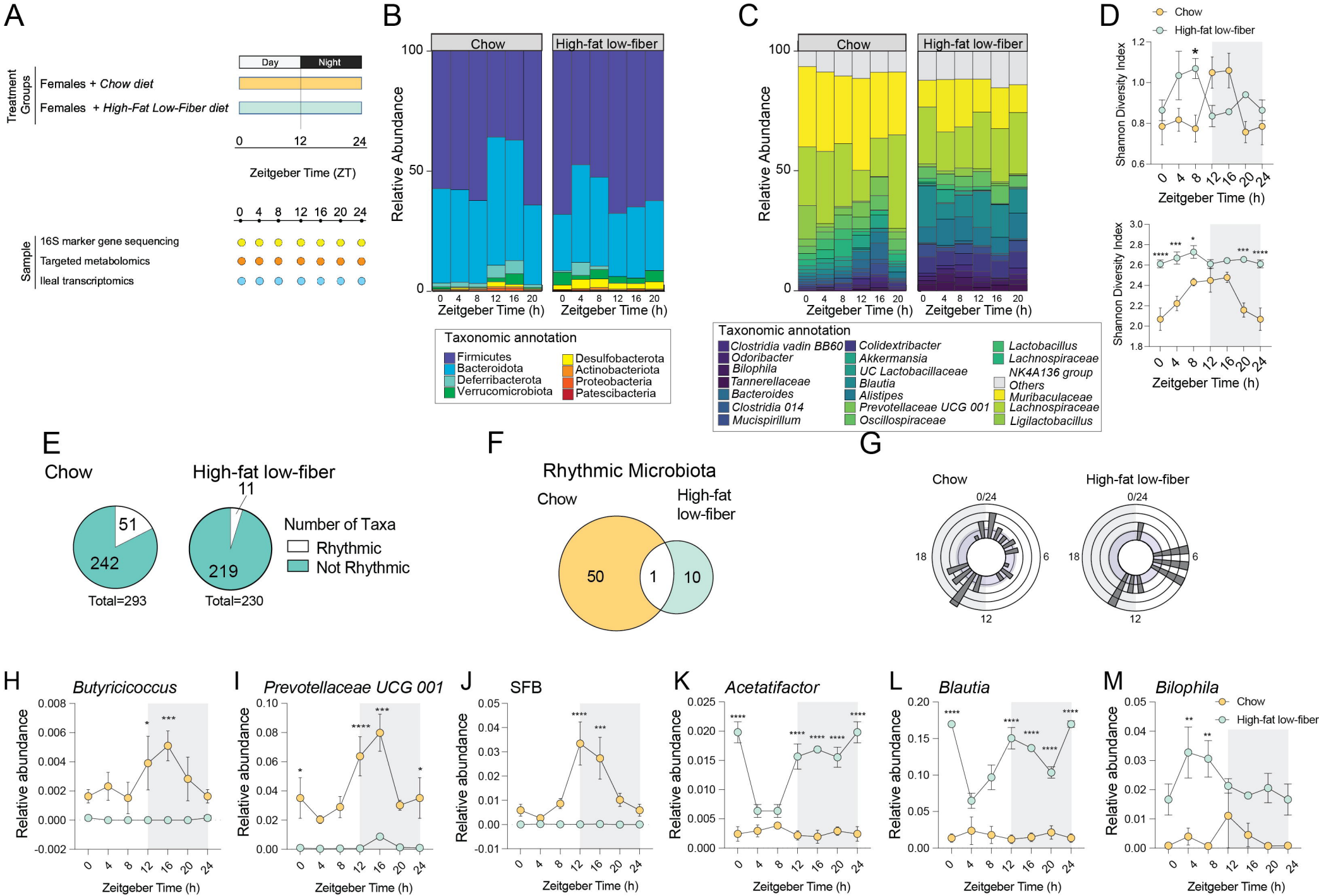
A
Treatment Groups
Females + Chow diet
Females + High-Fat Low-Fiber diet
Day
Night
0
12
24
Zeitgeber Time (ZT)
0 4 8 12 16 20 24
Sample
16S marker gene sequencing
Targeted metabolomics
Ileal transcriptomics
B
Chow
High-fat low-fiber
Relative Abundance
Zeitgeber Time (h)
Taxonomic annotation
Firmicutes
Bacteroidota
Deferribacterota
Verrucomicrobiota
Desulfobacterota
Actinobacteriota
Proteobacteria
Patescibacteria
C
Chow
High-fat low-fiber
Relative Abundance
Zeitgeber Time (h)
Taxonomic annotation
Clostridia vadin BB60
Odoribacter
Bilophila
Tannerellaceae
Bacteroides
Clostridia 014
Mucispirillum
Colidextribacter
Akkermansia
UC Lactobacillaceae
Blautia
Alistipes
Prevotellaceae UCG 001
Oscillospiraceae
Lactobacillus
Lachnospiraceae
NK4A136 group
Others
Muribaculaceae
Lachnospiraceae
Ligilactobacillus
D
Chow
High-fat low-fiber
Shannon Diversity Index
Zeitgeber Time (h)
E
Chow
High-fat low-fiber
51
242
Total=293
11
219
Total=230
Number of Taxa
Rhythmic
Not Rhythmic
F
Rhythmic Microbiota
Chow
High-fat low-fiber
50
1
10
G
Chow
High-fat low-fiber
0/24
6
12
18
H
Butyricicoccus
I
Prevotellaceae UCG 001
J
SFB
K
Acetatifactor
L
Blautia
M
Bilophila
Relative abundance
Zeitgeber Time (h)

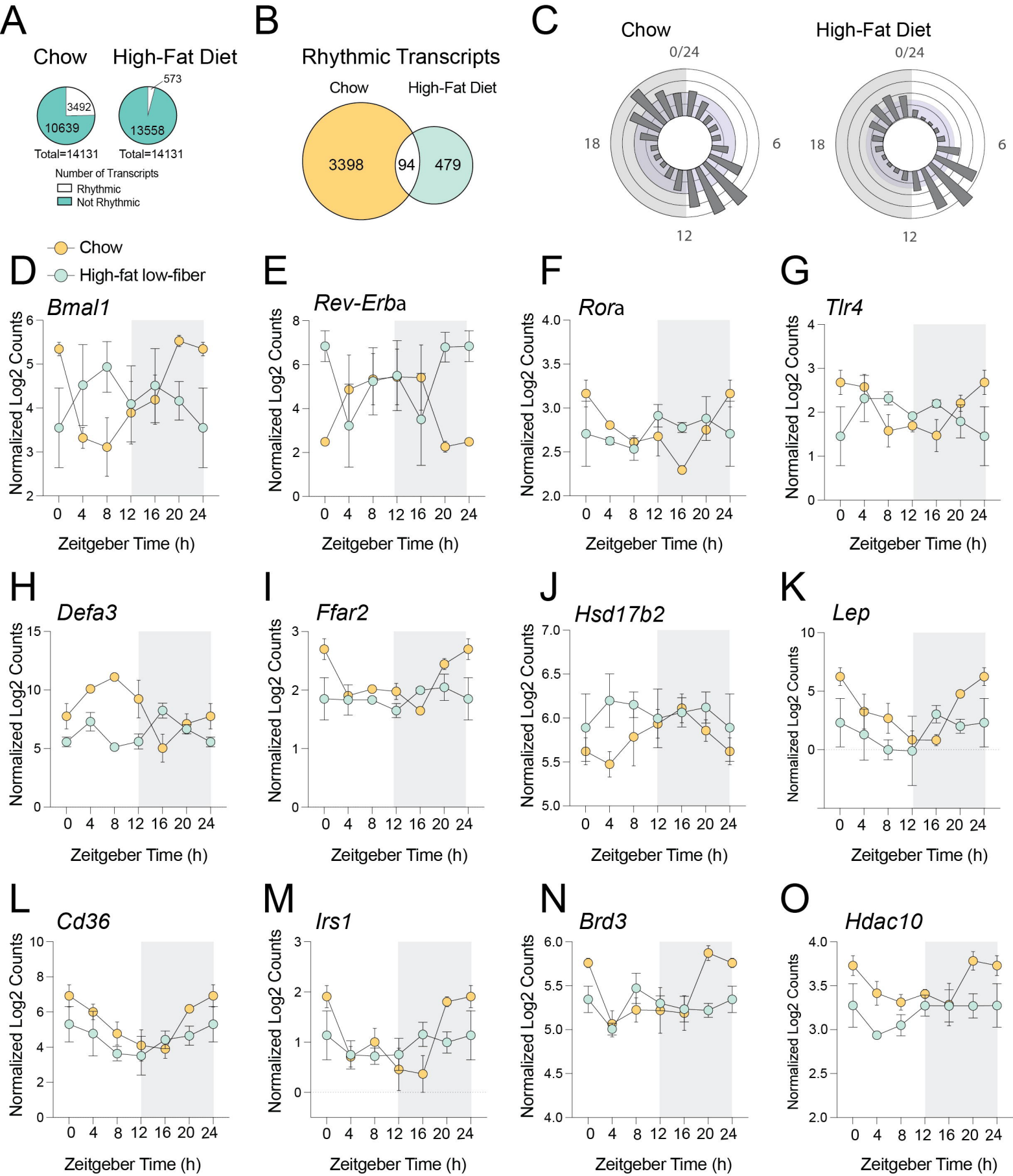
A
Chow
High-Fat Diet
3492
10639
573
13558
Total=14131
Total=14131
Number of Transcripts
Rhythmic
Not Rhythmic
B
Rhythmic Transcripts
Chow
High-Fat Diet
3398
94
479
C
Chow
High-Fat Diet
0/24
6
12
18
Chow
High-fat low-fiber
D
Bmal1
E
Rev-Erbα
F
Rora
G
Tlr4
H
Defa3
I
Ffar2
J
Hsd17b2
K
Lep
L
Cd36
M
Irs1
N
Brd3
O
Hdac10
Normalized Log2 Counts
Zeitgeber Time (h)